General Disclaimer

One or more of the Following Statements may affect this Document

- This document has been reproduced from the best copy furnished by the organizational source. It is being released in the interest of making available as much information as possible.

- This document may contain data, which exceeds the sheet parameters. It was furnished in this condition by the organizational source and is the best copy available.

- This document may contain tone-on-tone or color graphs, charts and/or pictures, which have been reproduced in black and white.

- This document is paginated as submitted by the original source.

- Portions of this document are not fully legible due to the historical nature of some of the material. However, it is the best reproduction available from the original submission.

A. & A. Book/ESSA

(NASA-CR-170855) CORONAL SOURCES OF THE INTRASTREAM STRUCTURE OF THE SOLAR WIND Final Report (Massachusetts Inst. of Tech.) 53 p HC A04/MF A01 CSCL 03B

N83-34875

Unclas
G3/92 36464

FINAL REPORT OF RESEARCH

Performed Under NASA Contract NAS8-33137

Coronal Sources of the Intrastream

Structure of the Solar Wind

Prepared for

George C. Marshall Space Flight Center

By

Dr. James D. Sullivan

Massachusetts Institute of Technology
77 Massachusetts Avenue
Cambridge, MA 02139

August 1983

Coronal Sources of the Intrastream Structure of the Solar Wind

Final Report of Research

Performed under NASA Contract NAS8-33137

Prepared for

George C. Marshall Space Flight Center

By

Dr. James D. Sullivan

Principal Investigator: Dr. Herbert S. Bridge

INTRODUCTION

The search for the solar source or origin of disturbances in the solar wind is a problem of continuing wide-spread interest dating from the firt measurements of the solar wind which showed high speed streams. Progress in understanding the specific relationships involved has accelerated since the launch of Skylab particularly with the identification of high speed streams as emanating from equatorial coronal holes (Kreiger et al., 1973, 1974; Nolte et al., 1976) and with the association of two high speed streams with the equatorial extension of the polar holes (Levine et at., 1977). However, the problem of direct identification of the solar source still remains for the lower speed solar wind in general and for structures in the solar wind variable on time scales < 4 days. Not surprisingly, several different mechanisms give rise to these solar wind structures.

In order to relate variable structures or fluctuations in the solar wind to coronal features, the use of subterrestrial point solar observations is dictated by the time scales involved. Using this approach, Sullivan and Nolte (1978) established a probable connection between a filament eruption and a small solar wind speed increase. The methodology used was to select a class of coronal transient events and to search for consequent disturbances of the solar wind.

The results found in this study on "Coronal Sources of the Instrastream Structure of the Solar Wind" were obtained by using an alternate approach of indentifying a class of structures in the solar wind, speed fluctuations within a high speed stream, and seeking to establish a connection with changes in the the solar corona, again at the subterrestrial point.

DATA SETS

Solar wind data were obtained from the MIT observations on IMP-7/8, hourly averages of the bulk proton parameter were used in this study. Solar corona data at the subterrestrial point were obtained from the ATM X-ray Spectrographic Telescope with varying time resolutions from 3 hours to 12 hours. In addition, for part of the study calculated field lines (Levine, 1978) were used to correct the correction point from the subterrestrial point to an estimated magnetic connection point.

METHODS AND PROCEDURES

The general analysis procedure was:

1) To identify good overlap periods between the data sets.

2) Within each overlap period to identify changes in solar wind speed (+100km S-1) within a high speed stream. This was normally near CMP (Central Meridian Passage) of a coronal hole. Each such change was called an event. This identification required the extrapolation of the solar wind data to a reference surface near the sun; a surface at two solar nadii was used.

3) For each event the X-ray observations were mapped to the reference surface; initially this mapping was simply radial, but later the potential field topology was used for a mapping along field lines.

4) To search for changes in the low corona a number of X-ray features which vary in time were examined. The list of X-ray features examined included transients, bright points, boundary shifts of coronal holes, area changes of coronal holes, etc.

5) From the list of possibly correlated events (X-ray and solar wind) we then tried to determine which coronal features best accounted for the observed intrastream structure. This analysis was guided by the twin criteria of longitude (and latitude) matching and the time duration of each event.

Results

The principal result of this study are summarized in the conclusion of E. Aslakson's Bachelor's thesis (Attachment A): "Short time scale changes in the bulk speed were found not to coincide with X-ray transients near the sub-earth point nor with the number of X-ray bright points within a coronal hole and near the equator. Instead, this study shows that the changes in bulk speed are associated with changes in light areas in a hole which may be associated with the opening or closing of magnetic field lines within the coronal hole. That there is a casual connection between these sudden changes (appearance or disappearance) in light area and sudden changes in the bulk speed of the solar wind is further evidenced by the spatial proximity on the sun of these changing light regions to the source position of stream lines from Levine's (1978) model that connect into the same solar wind streams."

This study also emphasizes the importance of continued monitoring of the region of the sun around the subterrestrial point with good time resoultion to have any prospect of unraveling the complex solar wind phenomena near earth (and also the need for continuous solar wind data). Limb observations are so time aliased as to have minimum value in understanding the variations in the solar wind on time scales of days.

Further progress in understanding the intrastream structure with the current data sets is possible but a really significant advance will require time continuous solar wind data and monitoring of the low corona at least every three hours. One hopes that, new observations in the current epoch of high speed streams will become available.

This study was chiefly performed by Eric Aslakson under the guidance of J. Sullivan (MIT), and D. Webb (AS&E). Extensive discussions with J. Nolte, A. Krieger, H. Bridge and A. Lazarus are gratefully acknowledged.

INTRA-STREAM STRUCTURE

OF

THE SOLAR WIND

by

ERIC RICHARD ASLAKSON

SUBMITTED TO THE DEPARTMENT OF PHYSICS
IN PARTIAL FULFILLMENT OF THE
REQUIREMENTS FOR THE DEGREE OF

BACHELOR OF SCIENCE

at the

MASSACHUSETTS INSTITUTE OF TECHNOLOGY

June 1982

Signature of Author _____
Department of Physics
December 10, 1981

Certified by _____
Alan J. Lazarus
Thesis Supervisor

_____
James D. Sullivan
Co-Supervisor

Accepted by _____
June Matthews
Chairman, Department Committee

TABLE OF CONTENTS

INTRA-STREAM STRUCTURE

OF

THE SOLAR WIND

by

ERIC RICHARD ASLAKSON

Submitted to the Department of Physics
on December 18, 1981 in partial fulfillment of the
requirements for the Degree of Bachelor of Science in
Physics

ABSTRACT

Changes of features in coronal holes observed from American Science & Engineering's (AS&E) X-ray telescope pictures were examined to find a possible cause of short time scale ($\leq$1 day) changes ($\pm$100 km/s) in the bulk speed of the solar wind observed by the MIT solar wind experiment on IMP-7 and 8 within a stream. X-ray bright points, X-ray transients, and changes in area and boundaries within and around five central meridian passages of two coronal holes were examined. In all, five coronal hole crossings were studied. Levine's (1978) calculated field lines were used to give an estimate of the longitude and latitude on the sun of the field line connecting with the earth.

The best correlation with the solar wind was a change in area of light regions within the coronal holes which occurred near the predicted magnetic field line connection point on the solar surface at the times that correspond to large changes in the bulk speed observed at the earth.

Thesis Supervisor: Dr. Alan J. Lazarus

Title: Senior Research Scientist

I. Statement of Problem

Since the observation of the effect of the solar wind on the magnetosheath from Explorer 10 (Bonetti et al., 1962), questions of its precise origin or driving mechanism have remained unresolved, especially the problem of the presumably different origin of the high and low speed wind in the corona. Progress in understanding the source origin of high speed solar wind streams with coronal holes. This was later verified by Nolte et al., 1976. In that study, high speed solar wind streams were found to emanate from the coronal holes, which are areas of decreased X-ray intensity in the solar corona, with low density and low temperature.

There are still questions about the origin of the lower speed solar wind (~300-400 km/s) and about short time scale variations (~ day) in the solar wind parameters. In this study, an attempt is made to identify short time scale changes in the bulk speed of the solar wind observed at the earth by the MIT solar wind experiment on the IMP spacecraft with specific features or changes in morphology within or near the coronal holes. During the flight of Skylab, in 1973, X-ray pictures, taken with the ATM S-054 telescope by American Science & Engineering, provided for the first time a detailed look at coronal holes and other features on the sun. These pictures were examined to see if any large-scale changes in area, bright point number, or transient activity could be associated with the short time scale variations in the solar wind.

II. Introduction

A. Description of Coronal Holes and Bright Points

Coronal holes are regions in the solar corona which begins at 1.03 $R_\odot$ and extends outward. They are regions of low density and temperature and low X-ray brightness compared to the surrounding coronal area. (Waldmeier,

1957, 1975; Newkirk, 1967; Altschuler et al., 1972.) They are most numerous in years immediately preceding the sunspot minimum. They are also known to exist in unipolar regions on the sun and have open field line topology. That is, the magnetic lines of force open into interplanetary space contrasting with most non-coronal hole areas where the lines are closed close to the sun. Open magnetic field lines emanate from the photosphere and extend to such heights that the dynamic forces of the outflowing solar wind exceed the restoring tensions and pressures of the magnetic field. The open structure partly accounts for the relative darkness of the coronal holes, since particles confined to field lines that are closed near the sun decelerate when they near the photosphere and emit X-ray radiation (see Figure 1).

As previously mentioned, coronal holes show a strong statistical association with high-speed streams in the solar wind and with geomagnetic disturbances on the earth (Krieger et al., 1973; Bell and Noci, 1976; Neupert and Pizzo, 1974; Hansen et al., 1976). One of the first clues to the existence of such special regions on the sun was the tendency for geomagnetic disturbances to have a 27-day period which is near the rotation period of the sun. The cause of the storms was thought to be intermittent long-lived streams of ionized solar material emitted from some specific region on the sun. This 27-day geomagnetic storm period was most prominent at the end of each sunspot cycle. These plasma emitting solar regions were named M-regions by Bartels in 1932, and have been of the perplexing problems of solar physics since then.

There were also visual investigations (by Waldmeier, 1957, 1975) who recognized persistent depressions in the intensity of the monochromatic

corona in ground-based coronagraphs. He called these areas "holes" (Löcher in German).

In the 1960's the knowledge of the solar wind grew from spacecraft measurements of its properties. As predicted by Parker, 1958, a solar wind of a continuous nature was observed.

During and after the Skylab mission (May 1973-February 1974, a period of declining solar activity and therefore high activity of holes) when observations in soft X-ray, XUV, vacuum-ultraviolet, visible, near-infrared, and radio wavelengths were made, the connection between high bulk speed solar wind streams and coronal holes was firmly made (Nolte et al., 1976).

Small (2×10^8 km^2) areas bright in X-rays are seen within coronal holes and are called bright points. They have an average lifetime of eight hours and exist outside coronal holes as well. By comparing their locations with a solar magnetogram, they are seen to be tiny bipolar magnetic structures. There emerge, on the average, 1500 X-ray bright points per day; and their areas correlate roughly with their lifetimes. By comparing bright point intensities at two wavelengths, Golub et al., 1974, have estimated the temperatures of the brightest bright points to be $1.3 - 1.7 \times 10^6$K and their densities to be two to four times higher than the coronal average.

B. Description of X-ray Transients

X-ray transients as defined by Webb et al., 1976, are a class of large-scale transient X-ray brightenings in the lower corona that are typically associated with the disappearance of Hα filaments. In Webb's study, he defined "large-scale brightenings" as all regions outside active regions having a brightness at least equivalent to the diffuse, large-scale

corona with a projected area on the solar disk ~10^{19} cm^2. These brightenings have a lifetime less than 30 to 40 hours and the associated Hα filament disappearances have lifetimes on the order of minutes to several hours with an average duration of four hours. After the Hα filament disappearance, there appeared in the same cavity an X-ray transient. In these brightening filament regions, there were apparent expansion velocities on the order of tens of km/sec and observed peak temperatures on the order of a few million degrees.

In a later work, Webb, 1978, confirmed a spatial association between the transients and neutral magnetic field lines. These neutral line occur over magnetic polarity inversion in the photosphere. Most of the transients were also related to large-scale changes in coronal hole areas. For this reason, the X-ray transients were investigated in this study as one of many possibilities for possible shaping of the intra-stream structure.

C. Description of ATM Telescope

The S-054 X-ray telescope is described by Vaiana et al., 1977; Giaconni and Rossi, 1960, were the first to propose the use of paraboloid mirrors for X-ray photographs. The S-054 telescope's primary optics is a nested pair of coaxial and confocal, grazing-incidence mirrors of paraboloid/hyperboloid design (see Figure 2). Its focal length is 213 cm with a geometrical area of 42 cm^2. The solar image produced is 1.9 cm in diameter and has a spatial resolution of 2". There is instrument scattering of very bright features by the grazing incidence mirrors that affects the quality of the images in regions near the very bright features in the corona. There were six different broad band filters available for the purpose of

looking at the corona in different X-ray wavelengths and different flux levels (see Table 1). There were also eight possible exposure times available.

Coronal hole boundaries are most apparent in the longest exposure time (256s) with the thinnest filter (passband 2-32 and 44-54 Å) because this combination allows one to see features that are faintly emitting. This combination allows one to see the features that are faintly emitting such as soft X-rays emitted from coronal plasma at temperatures slightly over a million degrees. At such temperatures, the pictures on "internegs" used in this study "look" into the region at the base of the corona (above 1.03 $R_\odot$).

The energy flux incident on the focal plane is given by:

$$I = \frac{A}{4\pi f^2} \int_0^\infty ne^2 \, dl \int_{\lambda_1}^{\lambda_2} P(\lambda_1 T_e) \, \eta \, (\lambda) \, d\lambda$$

where A is the telescope area, f is the focal length, n_e is the electron density, $P(\lambda_1 T_e)$ is the power at wavelength λ and electron temperature T_e of an emission whose integral is 1, η (λ) is the product of the filter transmission of the i^{th} filter and the telescope efficiency, and l is the path length along the line of sight. In the range of wavelengths that pass through the thinnest filter, $P(\lambda,T)$ is proportional to T^2. This means that the brightness of X-rays seen at the telescope is proportional to $n_e^2 \, T_e^2$ integrated along the line of sight. Coronal holes appear dark mainly because of their low density.

D. Solar Wind Data - Propagation Method and Levine's Solar Magnetic Field Model

The solar wind data used in this study were principally from the MIT IMP-7 & 8 spacecraft. These data were supplemented by data from other

experimenters including the Interplanetary Medium Data Book by Joseph H. King.

The solar wind data were projected to the sun using a radial, constant-velocity approximation. This technique is discussed by Nolte and Roelof, 1973, and was first used by Snyder and Neugebauer, 1966. The solar wind was propagated inward to a source height of 2 solar radii. To find the source longitude of the solar wind, the Earth-to-Sun distance is simply divided by the bulk speed as observed at the earth and the source longitude at the sun is then calculated. The reference height of 2 solar radii was chosen because of its closeness to the corotation height, which is the place with it and the plasma stops corotating. This method can, of course, only roughly predict the true source longitude because of uncertainties in the velocity of the solar wind less than 20 solar radii from the sun.

In this study Levine's model of the magnetic fields near the sun was used. If one assumes that the currents producing the magnetic field near the sun exist below the photosphere, then the magnetic field near the sun may be found by finding the solution to Laplace's equation:

$$\nabla^2 \psi = 0$$

in terms of a spherical harmonic expansion:

$$\psi(r,\theta,\phi) = R \sum_{n=1}^{N} \sum_{m=0.}^{n} \left(\frac{R}{r}\right)^{n+1} P_n^m(\theta) \left(g_n^m \cos m\phi + h_n^m \sin m\phi\right)$$

One solves for the coefficients g_n^m and h_n^m by applying boundary conditions at the photosphere and at a source surface at 1.6 solar radii. The boundary condition at the solar surface is obtained from daily magnetograms from Kitt Peak National Observatory. These magnetograms are line of sight measurements

of the magnetic field at the photosphere. These magnetic field measurements for a full solar rotation are averaged onto a synoptic grid containing 180 latitude bins with equal intervals of sin θ and 36° longitude bins. The magnetic field lines are perpendicular to the source surface at 1.6 solar radii. This supplies another boundary condition and a model of the magnetic field may be calculated.

III. Event Selection

Because of the large number of coronal holes crossing the central meridian (see Figure 3), it was necessary to restrict the number of crossings studied. The crossings studied are indicated in Figure 3. The central meridian passages (C.M.P.) of coronal hole 1 (CH1) in the Carrington rotations 1602, 1603, and 1604 were chosen because of the intra-stream structure seen in the bulk speed, i.e., short time scale (~1 day) variations in the bulk speed within a specific stream. Some examples of this intra-stream structure can be seen in Rotation 1602, Carrington longitude 30, in Rotation 1603, longitude 28°, and 5° in Rotation 1604, longitude 43°, and 23°. There are two types of coronal holes: those that are an extension of the North Polar hole, and those called equatorial holes, that are not connected to the polar holes. They have different characteristics especially in the variability of their enclosed area (Nolte et al., 1978). In order to study not only a polar hole such CH1, an equatorial hole, CH2, in Rotations 1606 and 1607 was also examined. Specifically, changes in the coronal hole corresponding to sudden changes in the bulk speed at longitudes 95 and 82° in Rotation 1606 and longitude 120, 90, and 80° in Rotation 1606 were sought.

Passages of coronal holes in Rotation 1609-1610 were not studied because of a limited number of X-ray images available during periods when there were

no astronauts in Skylab and, hence, poor time resolution. There were also gaps in the IMP data because the spacecraft was periodically in the magnetosheath or magnetosphere. Whenever those gaps occurred during the main crossing of the coronal hole, the crossing was not examined. Also, the crossings of mature coronal holes were chosen because of the difficulty in defining the boundaries of newly formed coronal holes.

Six crossings were chosen and they are marked in Figure 3. The X-ray pictures were also numbered. The frames used in this study and the times corresponding to each frame are given in Table 2.

IV. Summary of Procedure

A tracing paper was laid over the X-ray pictures or internegs and the boundaries within ~$\pm$70° (North and South, East and West) of C.M.P. of the coronal holes were marked. The bright points within the coronal holes that were $\pm$70° of C.M.P. and those outside the coronal holes within $\pm$20° of C.M.P. were marked on the overlays. A relative brightness scale with three brightnesses was used for the bright points. Also included on the tracing were any very bright or dark regions within ~$\pm$40° of C.M.P. These very bright regions were also given a relative brightness scaling of three. Any light areas within the coronal holes were also marked on the tracings.

The areas of coronal holes lying within 20°x20° and 40°x40° "windows" centered on the C.M.P. were then measured from the tracings and can be seen in Figures 4b, 6b, 8b, 10b,c, 12b. The area of light regions within the coronal holes and inside the windows was also calculated for each coronal hole. The number of bright points lying in these 2 windows were also counted and plotted. For some of the events, a movable window was used which was centered on the coronal hole and followed it as it traversed the solar disk.

For nearly every event, or the crossing of a particular coronal hole across the sub-earth point, the highest time resolution available was used to make the tracings. The best time resolution was the August crossing of CH1 with an interneg examined every three hours. In the other events, the highest available resolution was an interneg every 12 hours. A more complete description of the procedure may be found in the appendix.

V. Summary of Results

Following is a summary of the results given in the Appendix.

During the passage of CH1 in Rotation 1604, there was a sudden change in the bulk speed that mapped (using a radial, constant velocity approximation of the solar wind to two solar radii) to the sun at 18° Carrington longitude (see Figure 4a). The magnetic field line from Carrington longitude 18° at 1.6 solar radii (Levine's source surface) connects with the solar surface in a part of the coronal hole that underwent a sudden change in light area. This changing region is near Carrington long. 25 and lat. S5 and was light in interneg #25224, but five hours later in interneg #25298 it had darkened suddenly (see Figure 5a). The number of bright points in the 20°x20° and 40°x40° window made no difference in the change in bulk speed in this or later passage.

The passage of CH1 across the C.M.P. during Rotation 1603 had only one sudden change in the bulk speed corresponding to a Carrington longitude of 1° (see Figure 6a). There were no transients close to this time, and the changes of light area in the hole and boundary movements were small compared to the changes observed in other passages. There was an increase of light area near Levine's source position (about 2° distant) that could account for the change in bulk speed, although the magnitude of the area

change was not large. The changing area can be seen in interneg #21236 (see Figure 7a) at Carrington longitude 12.6, latitude S10. The uncertainty of the connection between this bulk speed change and the changing light area in the coronal hole on interneg #21236 is further increased by the long time between internegs.

The passage of CH1 during the Rotation 1602 had a sudden decrease in bulk speed corresponding to a Carrington longitude of 24° (see Figure 8a). The source position of this stream according to Levine's model lies in an area within the hole that changed from light to dark (-12 deg^2 area change at Carrington longitude 17, and latitude S5). This may be seen on interneg #20301 (see Figure 9a).

There were three sudden changes in the bulk speed observed during the Carrington Rotation 1607 passage of CH2 at Carrington longitude 122°, 90°, and 74° (see Figure 10a). The solar surface source location of the 74° stream existed directly beside a region in which a boundary change occurred (Carrington longitude 74° and latitude N15°). The 90° stream source location was in a region where light area within the hole changed to dark area and a shrinkage of the boundaries of the hole occurred at Carrington longitude 86° and latitude 12°. There was also a disappearance of light area in the hole at the same time as the change in the 122° stream.

There were two structures in the solar wind that were investigated during the 1606 passage of CH2. They were at 82.5° and 103° Carrington longitude (see Figure 12a). The source location of the 103° stream on the solar surface is at a point between the two parts or lobes of CH2 and coincides with the shifting of the boundaries as seen in internegs #40524-40540 (see Figure 13a). The source location for the stream at 82.5°

Carrington longitude is in the upper left lobe of CH2 which was relatively stable at that time.

VI. Conclusion

Short time scale changes in the bulk speed were found not to coincide with X-ray transients near the sub-earth point nor the number of X-ray bright points within a coronal hole and near the equator. Instead, this study shows that the changes in bulk speed are associated with changes in light areas in a hole which may be associated with the opening or closing of magnetic field lines within the coronal hole. That there is a casual connection between these sudden changes (appearance or disappearance) in light area and sudden changes in the bulk speed of the solar wind is further evidenced by the spatial proximity on the sun of these changing light regions to the source position of stream lines from Levine's (1978) model that connect into the same solar wind streams.

VII. Appendix

A. Procedure

Following is an explanation of the method used to determine the changes of shaded and dark areas in the coronal holes studied. Because of the need to compare many different pictures of the sun that were separated from each other by three to twelve hours and the difficulties in achieving an absolute measure of intensity due to differences in developing and scattering of light in the corona, it was decided that the X-ray pictures should be compared without a densitometer.

A Carrington heliographic longitude and latitude system, or Stonyhurst grid was overlaid on the X-ray picture. A tracing paper was then set over

the combination of X-ray picture and Stonyhurst grid and the boundary of the coronal hole was drawn.

Also included on these tracings were bright points and "active regions" or very bright areas ($100^{\circ 2}$ in area). In addition, any area which appeared light or shaded within the coronal hole was also marked. Often these lighter areas within the coronal hole included bright points and often they reached to the boundaries of the coronal hole.

Occasionally, it was a matter of some debate where the exact boundary of the coronal hole should be drawn and whether one should define light area next to the boundary as being in or out of the coronal hole. This problem was worse with the crossings of CH2 examined. Its boundaries were less well defined than in the CH1 crossings.

In order to lessen the effect of the possibility of difference in the judged intensities, each event or passage of a coronal hole completed at the same sitting. An effort was also made to compare the boundaries and intensities of later pictures with earlier ones during the same day in order to achieve some degree of consistency. If it was not possible to do a complete crossing of a coronal hole in one sitting, the previously drawn boundaries for this hole were reexamined at the next time sitting. The boundary for one of the events was also checked by having another person determine them independently. The agreement was good with the earlier boundaries.

The bright points in the area within and around the coronal hole were classified in a three-level system: X as most bright, V as less bright, and - as barely visible. If a bright point occurred at the edge of a coronal hole, it was not counted as being in the coronal hole. During the

August 9 crossing of CH1, each individual bright point was followed from picture to picture; but otherwise, the points were simply counted within longitude and latitude regions. The bright points in CH1 were found to last on the order of 9 hours in close agreement with Golub et al., 1974.

The active regions were also classified in a three-level system: 3 as bright, 2 as less bright, and 1 as barely visible. If X-ray transients, as defined by Webb, 1976, existed near the time or source longitude of the solar wind streams studied, they were also considered as candidates for contributing to the intra-stream structure. Long regions of light and dark near the coronal hole sometimes corresponding to X-ray transients were also marked on the tracing paper.

Within the coronal holes there often appeared regions that were not as bright as the area outside the boundary of the coronal hole but were definately lighter than surrounding regions within the coronal hole. In this study, these light regions within the hole will be referred to as light area. The other dark regions will be called dark area. The boundaries

of these regions were marked on the tracing paper and lt. and dk. were written to distinguish the different areas within the hole. An example is given above.

Once the maps were drawn, they were overlaid with another Stonyhurst grid with 2-degree separations between longitude and latitude lines. The areas of the dark and light regions in the coronal holes were tabulated in unit of square degrees of solar surface area. The area was calculated to within one square degree. The area which was examined was determined in two ways: the first was with a square "window" centered on the sub-earth point and extending $\pm$10° from that point, i.e., the window was fixed and the coronal hole was observed as it passed underneath. The second method followed the coronal holes across the solar disk by taking all of the area within a $\pm$10° band of latitude.

The number of bright points within a 20°x20° square window and also within a 40°x40° square window both defined by the first method. Bright points with brightness of - were not counted. Any X-ray transients from the list given in Table 3 were marked on the area vs. time graphs (see Figures 4, 6, 8, 10, 12b,c).

After all of the light and dark areas within the coronal holes using both methods and the number of bright points were calculated, times when there were large changes in the areas, or eruptions of X-ray transients, or sudden increase of bright points were more closely examined. In the case of the area calculations, the specific changes in the hole responsible for changes in the area were examined. These locations of changing area were also compared with Levine's 1978 predictions of solar surface longitude and latitude of solar wind reaching his source surface to see if they coincided. This coincidence would give a stronger hint that the

areas actually influenced the solar wind. The locations of X-ray transients were also noted and taken into account.

B. Results

In this section the crossings of the individual coronal holes across the central meridian passage (C.M.P.) that were examined in this study will be discussed.

The crossing in Carrington Rotation 1604 of coronal hole 1 (CH1) will not be considered. As one can see in Figure 4a, there are two structures in the delayed solar wind bulk speed versus solar source longitude that bear investigation. One can see sharp decreases in the bulk speed at 18° and a smaller increase at 2° long. One must bear in mind that these longitudes are only approximate due to inherent difficulties in the delay method. One such difficulty is stream-stream interactions between the sun and earth that accelerates the solar wind, especially the wind at the beginning of a high speed stream. There is also a sharp increase at 44° long., but this probably not associated with CH1 since it is well past its boundaries and even exists very near or on the other side of a sector change in the magnetic field.

CH1 on interneg #25224, August 20, 2003 GMT appeared as in Figure 5a. CH1 was the longest lived coronal hole during the Skylab mission aside from the polar holes. It lasted from Carrington Rotation 1601 to 1607. It existed in a positive magnetic cell reaching from the north pole and as such, was an extension of the north polar hole.

During this rotation, the boundaries of the coronal hole at the ecliptic equator stretched from 16° to 32° Carrington longitude. The bright point #6 in Figure 5a later developed into a very bright region within the coronal hole one quarter solar rotation later than this interneg.

There were also two X-ray transients in the vicinity of this hole. From the table from Webb et al. (1976) of X-ray transients (see Table 3) within ±15° of C.M.P., we see transients on August 18 and August 24. Only the transients near the passages considered in this study will be given.

The first of these transients was too far south to be considered a possible source of the structure in the bulk speed, but the second is rather near the coronal hole. Even though it is near the coronal hole, it is also most likely not responsible for the change in the bulk speed since it is first visible August 24 which is 2-3 days after the projected change in bulk speed and since the lifetimes of X-ray transients are on the order of hours (Webb et al., 1976).

A plot of the area within a 20°x20° window centered at the sub-earth point and the number of bright points with brightness 2 or 3 within a 20x20 and 40°x40° bin is to be found in Figure 4b. There is a large increase in dark area at interneg #25298. This change occurred when the Carrington longitude of the sub-earth point was very near 18° which suggests a connection with the change in bulk speed at this longitude. Looking at the graph (see Figure 4c) of the total area of the coronal hole in a band of longitude within ±10° latitude versus longitude of the C.M.P. for that interneg, one sees this same increase of dark area at interneg #25298. There are also increases of dark area on interneg #25496 and #24870 and slow decreases in the light area in #24990-25107 and #25388-25420. Some of these changes are caused by a mixture of boundary changes and inner shaded region changes and some are caused by either a change in boundary or a change in inner shaded area. These changes are summarized in the following table.

Interneg	CH Boundary Change			Changes of Area in CH		
	Area (deg^2)	Location (deg)		Area (deg^2)	Location (deg)	
		lat.	long.		lat.	long.
24990-25107	---	---	---	+56	-10 to 10	0 to -10
24825-24870	10*	8 to 12	0	-15	8	-18
	6	3	-5	-8	-6	-8
				-4	-6	-16
25224-25298	48	-6 to 6	16	-48	-3	6
25368-25420	-20	-1	27	-13	5	12
25420-25496	8	2	25	-64	-4	17
25496-25583	---			28	-4	25

*The new area is dark.

The coordinates of the changing area in this table will be given relative to the point defined by the intersection of the sub-earth longitude and the solar equator. A negative latitude means south of the equator, and a negative longitude means left (east) of the sub-earth longitude. A positive change of area will be taken to mean the appearance in the coronal hole of a light region. These conventions will be followed in this appendix unless otherwise stated by indicating, for example, 22°N Carrington longitude in which case the longitude refers to the Carrington system.

When an area change is given between two internegs, i.e., #25496-25583, the position of the changing-area is given in terms of the coordinates of the later interneg.

The farther that one gets from the center of the coronal hole passage in interneg #25224, the less effect any changes should have on the solar wind

since they are so far separated from the coronal hole and from the source of the solar wind (assuming a flow where the magnetic field lines bend little near the solar surface). Also, the error in the area measurements grows because of projection effects near the limb and instrument resolution (see Description of ATM Telescope). In other words, the areas in Figure 4c should most accurately reflect or signal changes in the solar wind for area measurements near the center of the graph. The reason that the changes in area in internegs #25496 and #24870 in Figure 4c are not visible in Figure 4b is that they occurred outside the 20°x20° set window used to make Figure 4b. It is interesting to note that the sub-earth point longitude for #25496 and #24870 is 11° and 32° respectively. There is, unfortunately, a data gap in the solar wind data at 11°. As stated before, the boundary of the hole is at (16°-32° longitude) and the change in the hole responsible for this small increase in the dark area is the disappearance of light area mostly at the left-hand side (east side) of the hole. This is the furthest side of CH1 from the sub-earth point and one could therefore expect that the connecting stream line is therefore not affected. This stream line assumption also fits with the calculated stream lines by Levine (1978) who shows the connecting longitude of the stream line intersecting his source surface at 30° (and therefore seen at the earth as if the stream originated near 30° connecting with the sun's surface at 27°. This is on the right-hand side of CH1 and therefore might not be affected by a change on the outer side of the coronal hole. Levine's model predicts connection points of field lines at the solar surface very near the equator so the window at $\pm$10° latitude is probably well placed.

In summary there are two times when the dark area in the hole is seen to increase drastically. They are at #25224-25298, where a large increase of dark area (48 deg^2) at long. 6, lat. -3 occurred, and at #25420-25496 where a large increase of dark area (+64 deg^2) at long. +17, lat. -4 occurred. The change in area in #25420-25496 occurred at a time that falls in a data gap in the solar wind data. There is a decrease of light area in interneg #25831 that could correspond to the sudden change at 2° Carrington longitude. Since the boundary of the hole is at 13° Carrington longitude, this change occurs when the stream line connecting the solar surface at this point and the earth is very non-radial. This can be seen in the Levine's model. Below is given one particular field line that connects to the earth at a time corresponding to a longitude of 4°. It is given at six intermediate points between the source surface and the solar surface. θ is the angle from the north pole, ϕ is the Carrington longitude, and R is the distance from the sun expressed in solar radii.

R	θ	ϕ
1.6	94.00	4.00
1.36	96.21	8.76
1.31	97.02	10.05
1.26	97.77	11.06
1.21	98.41	12.04
1.00	103.27	15.32

The change in area in #25224-25298 occurs near the connection point in Levine's model.

R	θ	Φ	R	θ	Φ
1.6	84.00	16.00	1.6	94.00	20.00
1.38	84.18	16.98	1.38	94.65	20.45
1.32	84.23	17.26	1.32	94.87	20.78
1.26	84.35	17.73	1.26	95.01	21.32
1.21	84.46	17.99	1.21	95.04	21.95
1.00	83.67	17.23	1.00	97.93	22.88

The sub-earth longitude for interneg #25224 is 20° and thus the connection points of the stream showing the sudden change in bulk speed lie in the changing area. It should also be pointed out, that the change in area observed after #25224 at 18° Carrington longitude that is perhaps responsible for the change of 150 km/sec in the bulk speed is roughly comparable to the velocity of stream versus coronal hole area figure observed by Nolte et al. (1976). In this study the total area of coronal holes and solar wind velocity for all of the coronal holes observed during Skylab were included. Nolte et al. found an empirical relationship between the area and velocity,

$$V = (80 \pm 2)A + 426 \pm 5$$

where A is the area in 10^{10} km^2 and V is the km/sec. From this, one can get

$$\frac{dV}{da} = 1.184$$

where a is in square degrees. This means that the area change in #25224-25298 implies a change in velocity of 56 km/sec.

The 1603 crossing of CH1 is shown in Figure 6a. There is a small increase (50 km/sec) at 1° Carrington longitude. CH1 in 1602 appeared as in Figure 7a on 24 July, 14:12 in interneg #21204. There was a persistent bright area in the hole where the 3 brightness is shown. There was also a light shaded area usually containing bright points at -10 (relative long.

and lat.) that was almost a constant feature of the hole. There was also a large shaded region (area 42 deg^2) at northern latitudes (+15) that, after a boundary change, caused a shrinkage of the width of the hole in the north. At the ecliptic equator, however, the width of the hole remained a constant 12 degrees (±1 degree). Except for the light area in the north, this was probably the most stable hole observed as far as boundary motions are concerned. Levine's model shows the field lines in the ecliptic plane connecting at equal latitudes on the sun or perhaps bending a little into the southern hemisphere for this passage.

R	θ	φ	R	θ	φ
1.6	86.00	24.00	1.60	86.00	16.00
1.39	86.05	22.40	1.38	86.13	16.07
1.32	86.10	21.87	1.32	86.16	16.19
1.27	86.21	21.49	1.26	86.30	16.44
1.21	86.32	21.06	1.21	86.58	16.74
1.00	86.12	20.83	1.00	86.67	17.19

There were three X-ray transient events that occurred near this crossing. They are shown in Table 3 and occurred on July 20/21, 21/22, and July 27. The X-ray transients on July 27 and July 20/21 were 30-40 degrees away from the closest edge of the coronal hole and the transient on July 21/22 could have been a candidate for affecting the solar wind except that it was too far north.

The areas in Figure 6b and c are seen to be very smooth with no large changes. As mentioned before, there is an increase in light area in the hole at northern latitudes (#21156-21188) and following this a decrease in total area at #21[illegible] along with a boundary change (area -24 deg^2) in the left-hand boundary in #21236. The change is along the left-hand boundary

from latitude -12 to lat. +4. This occurs at a Carrington source longitude 7°. At interneg #21236-21244, there was a decrease in the area of the light region inside the hole. Levine's field lines are given below for this period.

R	θ	φ	R	θ	φ
1.6	86.00	0.00	1.6	86.00	8.00
1.35	87.11	6.43	1.38	86.27	9.12
1.26	87.71	7.65	1.32	86.40	9.94
1.21	88.25	8.16	1.27	86.53	10.73
1.00	92.95	9.22	1.22	86.65	11.51
			1.00	86.69	16.47

The sub-earth longitude of #21236 was 7.63 and #21244 was .77° as can be seen in Table 2. The connection point on the solar surface for #21236 is at long. 8.5, lat. 0, relative coordinates on interneg #21236. The connection point for #21244 lies at the left-hand boundary -6° to the south. It is possible that the decrease in bulk speed at 1° Carrington longitude is due to this expansion of the light region that lay to the south of the equator at long. 5, lat. -10 on interneg 21236, although one would have expected the change to appear in the bulk speed a couple degrees earlier.

A complicating factor during this passage has the poor time resolution of the X-ray internegs. There was, however, no large sudden change in the bulk speed and also no large change in light area within the hole near Levine's source positions.

The next crossing to be considered was the 1602 crossing of CH1. As can be seen in Figure 8a, there is a large increase and decrease in the bulk speed at 24°. Coronal hole 1 appeared in interneg #20301 as shown in Figure 9a. At this time, CH1 had boundaries on the equator of 1.9° and 27.9°. There was an X-ray transient at long. 13, lat. -13 of X-ray importance 2

Webb, 1976). It can be seen on interneg #20301 as the bright area (labeled 3X). It seems possible that the transient at long. 13, lat. -13 could have an impact on the solar wind; however, when it exploded, it would not contribute matter to a stream line that would intercept the earth. As the coronal hole when by the sub-earth point, this transient was steadily decreasing in brightness. A plot of the area within a 20° x 20° window centered at the sub-earth and the number of b.p.'s within this 20° x 20° and a 40° x 40° bin are given and may be found in Figure 8b. A graph of the area within ±10° lat. may be found in Figure 8c. A list of the changes in CHl responsible for these area changes in Figure 8c and b will be given in the following table.

The biggest increase of light area is in #20301. This comes about partly from a +18 deg^2 boundary increase at the right edge of the hole and fluctuations about the boundary of the light area within the hole. Later, part of this area disappears in #20309.

Levine's field line intersecting the source surface at 24° Carrington longitude is given below.

R	θ	Φ
1.60	89.00	24.00
1.39	89.57	22.32
1.33	89.84	21.48
1.27	90.23	20.71
1.22	90.65	19.97
1.00	94.12	16.97

It can be seen in Figure 9a that this intersects interneg #20301 at relative long. -1, lat. -3. It is marked on 20301 and 20277 with an X. This particular location changes from light to dark in #30377-20301 with an area change -12 deg^2.

There are several possible explanations for the decrease in bulk speed. It is possible that the magnetic field line that shows the change in bulk speed came from a dark region in the hole that later (in 20277) changed to a light region. This region later turned dark. What is clear, however, is that there is a change of a light region in the vicinity of Levine's source position for the time when there is a sudden change in the bulk speed.

Interneg	CH Boundary Change			Changes in Area in Coronal Hole		
	Area	Location		Area	Location	
		lat	long		lat	long
20245-20269	+16	at left boundary		+112	-10 to 20	-4
20269-20277	+20*	-8	-20			
		-12 to -26		-34	near right boundary	
20277-20301	+16	at left boundary		-12	8	0
		8	-8	+8	14	0
	+18	at right boundary		+8	-8	-2
				+13	8	4
				+12	9	-4
20301-20309	-32	at right boundary		-8	4	4
				-8	-6	2
20309-20341	-35	at left boundary		+4	0 to 8	12

*The new area is dark.

The next event considered will be the 1607 crossing of CH2. There were several relatively short time scale changes in the solar wind. There were three sudden decreases in the bulk speed at 122°, 90°, and 74° (see Figure 10a). CH2 appeared as in Figure 11a, in 41434 during Rotation 1607.

It was an equatorial hole and existed in a negative polarity magnetic sector. Its boundaries were generally defined less clearly than in CH1 and it was generally harder to be consistent in the determination of the light area within the hole.

There were no X-ray transients nearer to CH2 than 48° N-S or E-W during this rotation. The area in a 40° x 40° window is given in Figure 10c. For this crossing, the area in a 10° band around the ecliptic equator was not calculated. The area in a ±10° band of latitudes was not helpful because the coronal hole was so long in longitude with separation between its individual parts. If the stream lines connect at a certain point within the hole, then taking the whole area over a large range in longitude would be as unhelpful as taking the area over a large range in latitude, since the area plots are only used to see large changes in the light or dark areas and then these internegs in which areas changed are examined to see what specific changes occurred. The 40° x 40° window was used because of the position of this hole in the northern hemisphere.

There were two times when there was a sudden increase in dark area due to the disappearance of light area and one time when a sudden boundary change occurred decreasing the dark area. These can be seen on internegs 41402, 41490, and 41506, respectively. Other changes in CH1 will be summarized in the following table.

The change of area in #41378-41402 was mainly a disappearance of light area that existed in the hole. The change of area in #41466-41490 was also a disappearance of small regions of light area within the hole. Levine's field lines of these two sets of internegs are given below. The connection

Interneg	CH Boundary Changes			Changes in Area in CH		
	Area (deg^2)	Location (deg)		Area (deg^2)	Location (deg)	
		lat	long		lat	long
41378-41402				-10	18	-14
				-13	18	0
41466-41490				-8	11	3
				-16	12 to 22	-4
				-4	11	-2
41506-41522	+28*	4 to 10	6 to 12			

*New area is dark.

points on the solar surface of the stream lines with sudden changes in bulk speed are marked in the corresponding internegs (41466 and 41522) with stars. These points are near or at the locations that there are changes in light area in 41466 and changes in boundary in 41522.

R	θ	ϕ	R	θ	ϕ
1.60	85.00	88.00	1.60	85.00	72.00
1.38	84.11	88.61	1.36	80.89	74.87
1.32	83.58	88.67	1.30	80.09	75.31
1.26	82.95	88.63	1.25	79.24	75.65
1.21	82.24	88.38	1.00	75.18	74.80
1.00	77.83	85.82			

To summarize, the solar surface source locations of the streams at 90° and 94° Carrington longitude be in regions in which there are boundary changes or changes of light to dark area. There are also changes in area of light regions in CH2 that could correspond to the stream at 122° Carrington longitude.

The crossing of CH2 in Rotation 1606 is shown in Figure 12a. There was a sharp decrease of the bulk speed at 82.5° and 103° long. CH2 appeared

as in Figure 13d in interneg #40596. There was an X-ray transient on October 8/9, 01:23. It is the lightish (1) region to the south of the lower part of the coronal hole on #40596. It is far to the south and did not explode until it was around 11° to the right of the central meridian, and it is possible that it affected the solar wind. It is marked with an X on Figure 12b.

The area in a 20° x 20° window is shown in Figure 12b. The specific changes in the hole within a 20° x 20° window responsible for the changes in the graph are listed in the table below. The band of longitudes within ±10 latitude method of calculating areas was not used here because of the length of the hole in longitude.

Just as during the 1607 crossing of CH2, the boundaries of this hole were very changeable. This was partly due to the time resolution of the X-ray pictures but also because of the changeable characteristic of the equatorial holes during the Skylab period. It was not not as easy during the passages of CH2 to map the boundaries as it was for the passages of CH1. There were times during this passage, when the coronal hole separated itself into two parts.

According to Levine's predictions, the connection point for the field line at 100° is near the place where there is a boundary change in #40524, and later the connection point moves up to higher latitudes into the region

R	θ	φ	R	θ	φ
1.60	94.00	100.00	1.60	94.00	108.00
1.39	92.67	100.84	1.38	93.25	108.20
1.33	91.67	100.93	1.32	92.73	108.46
1.28	90.49	100.98	1.26	92.04	108.59
1.23	89.52	101.41	1.21	91.41	108.90
1.00	86.17	104.61	1.00	89.97	110.14

in the center of the large upper left lobe which was relatively stable. Thus, when there is a big area change at #40596, it is possible that it does not affect the solar wind due to the fact that the changing area responsible for the change in area is located in the lower connection region between the two parts of CH2.

θ	ϕ	R
74.00	84.00	1.60
89.88	85.68	1.35
88.69	86.06	1.29
87.48	86.09	1.24
86.17	86.18	1.20
80.29	83.40	1.00

Interneg	CH Boundary Changes			Changes of Area in CH		
	Area (deg^2)	Location (deg)		Area (deg^2)	Location (deg)	
		lat	long		lat	long
40476-40508	none			none		
40508-40524	-49	-3	0			
	+28	-10	0			
40524-40540	-32	0 to -4	-8 to 2			
		-6 to -10	2 to 9			
		(upper boundary of lower part of hole)				

In interneg #40556-40596 there is a separation of the 2 parts of CH2 at lat. 0, long. 5. The upper part of CH2 is during the time of these two internegs relatively stable.

C. Carrington Longitude and Latitude

The Carrington longitude and latitude of the sub-earth point on the sun was needed to connect the delayed solar wind data with the X-ray pictures of the sun which had coordinates in Carrington longitude. A subroutine was written to give this sub-earth point in Carrington longitude and latitude. In Carrington's h(iographic system, an arbitrary starting point was chosen for the zero meridian. Carrington's zero meridian passed the ascending node of the solar equator January 1, 1854 at zero hours, Greenwich time. This heliographic system rotates with a defined sideareal period of 25.38 mean solar days. The synodic period which is the time between successive zeros of the Carrington longitude at the sub-earth point is 27.2753 days.

Referring to Figure 14, one knows from Kepler's second law,

$$\frac{\text{Area SPA}}{\text{Area of ellipse}} = \frac{t - T}{T}$$

$$\text{Area SPA} = 1/2\ n\ a\ b\ (t - T),$$

where $n = \frac{2\pi}{T}$ and T is the period of rotation and t is the starting time, a and b are the semi-major and semi-minor axes respectively.

We next define a circle tangent to the ellipse at the perihelion A and aphelion B with radius A and extend A perpendicular to the major axis AB through P to a point on the Circle Q.

The angle QCA is the angle E and is called the eccentric anomaly. The PSA is the angle U and is called the true anomaly. γ is the direction of the vernal equinox and points in a direction in an inertial frame that is almost constant.

According to a property of ellipses,

$\frac{PR}{QR} = \frac{b}{a}$, expressing PR and QR in terms of V and E, one gets

r sin V - b sinE, SR = CR-CS = a cosE-ae

where e is the eccentricity or

$$r \cos v = a (\cos E - e)$$

squaring x and y and adding, noting that $b^2 = a^2 (1-e^2)$, we obtain

$$\tan \frac{V}{2} = \left(\frac{1+e}{1-e}\right)^{1/2} \tan \frac{E}{2}$$

Careful examination of the areas in Figure 14 establish a relation between the eccentric anomaly and the mean anomaly defined as,

$$M = n(t - \tau) \text{ where } n = \frac{2\pi}{T}$$

this relation is known as Kepler's equation and is,.

$$E - e \sin E = M$$

where E and M are in radians. Since e << 1, this equation is solvable by a recursive method.

Referring to Figure 15, one sees that N and N' are the ascending and descending nodes respectively, and if γ is the direction of the vernal equinox, and if A is the perihelion, then angle ASP is the true anomaly v. The arc NA., measured from the ascending node to the perigee is called w. The arc γN is the longitude of the ascending node and is denoted by θ. The sum of the two arcs NA and γN is the longitude of perihelion and is denoted by $\bar{\omega}$. Finally, the true longitude $L = \omega + v = \bar{\omega} + v$.

The values of the mean longitude of perigee, the mean anomaly, and the eccentricity are given in the Explanatory Supplement to the Astronomical Ephemeris and American Ephemeris and Nautical Almanac, pg. 98, and the longitude of the ascending node of the solar equator on the ecliptic (Ω) and the heliographic longitude of the node of the equator (M) are given on

pgs. 307-308. Examining the Figure 16 where E is the sub-earth point and Lo and Bo are the heliographic longitude and latitude of the sub-earth point on the sun, one can form a spherical triangle. In this triangle,

$$\tan (Lo - M) = \tan (\lambda - \Omega) \cos I, \quad \sin B = \sin (\lambda - \Omega) \sin I$$

where I is the inclination of the equator with respect to ecliptic, and λ is the geocentric longitude of the sun.

If λ denotes the geocentric longitude of the sun, then $\gamma E = \lambda + 180°$. From these relationships, one can find the longitude and latitude of the sub-earth point on the sun as a function of time. Table 4 contains the Fortran subroutine written to calculate these parameters.

Acknowledgement

I would like to express my sincere thanks to Dr. James D. Sullivan for the many hours of help, suggestions, feedback and encouragement he gave me during the writing of this thesis. My thanks to David Webb of American Science and Engineering for his guidance in helping me to use and interpret the x-ray data. To Dr. Alan J. Lazarus my thanks for his suggestions and careful proofreading. My thanks, also, to the entire Solar Wind Group for their helpfulness and encouragement, including Professor Stanislaw Olbert for the many hours spent teaching me. To Joan Boughan, Anne Bowes, Pamela Milligan and Mary Terkoski my thanks for all their help. This work was supported in part by Contract NAS 5-27590.

VIII. Bibliography

1. Levine, Randolph H., The Relation of Open Magnetic Structures to Solar Wind Flow, JGR 83, No. A9, September 1, 1978.
2. Krieger, A. S., A. F. Timothy, and E. C. Roelof, A Coronal Hole and its Identification as the Source of a High Velocity Solar Wind Stream, Solar Physics 29, 505, 1973.
3. Nolte, J. T., A. S. Krieger, A. F. Timothy, R. E. Gold, E. C. Roelof, G. Variana, A. J. Lazarus, J. D. Sullivan, P. S. McIntosh, Coronal Holes as Sources of Solar Wind, Solar Physics 46, 303-322, 1976.
4. Waldmeier, M., Die Sonnenkorona, Vol. 2, Verlag Birkhauser, Basel, 1957.
5. Waldmeier, M., The Coronal Hole at the F March 1970 Solar Eclipse, Solar Physics 40, p. 351, 1975.
6. Newkirk, G. A., Structure of the Solar Corona, Ann. Rev. Astron. Astrophys. 5, 213, 1967.
7. Altschuler, M. D., D. E. Trotter, and F. W. Orall, Coronal Holes, Solar Phys. 26, 354, 1972.
8. Bell, B. and G. Noci, Intensity of the Fe XV Emission Line Corona, the Level of Geomagnetic Activity, and the Velocity of the Solar Wind, JGR 81, 4508, 1976.
9. Neuport, W. M. and V. A. Pizzo, Solar Coronal Holes as Sources of Recurrent Geomagnetic Disturbances, J.Geophys.Res. 79, 3701, 1974.
10. Hansen, R. T., S. F. Hansen and C. Sawyer, Long-Lived Coronal Structures and Recurrent Geomagnetic Patterns in 1974, Planetary Space Science 24, 381, 1976.

11. Parker, E. N., Dynamics of the Interplanetary Gas and Magnetic Fields, Astrophys. J. 128, 664, 1958.

12. Golub, L., A. S. Krieger, J. K. Silk, A. F. Timothy, and G. S. Variana, Solar X-Ray Bright Points, Ap. J. 189, L93-197, 1974.

13. Webb, D. F., A. S. Krieger, D. M. Rus, Coronal X-ray Enhancements Associated with H= Filament Disappearances, Solar Phys. 48, 159-186, 1976.

14. Webb, D. F., P. S. McIntosh, J. T. Nolte, C. V. Solodyna, Evidence Linking Coronal Transients to the Evolution of Coronal Holes, Solar Phys. 58, 389-396, 1978.

15. Giacconi and Rossi, B., A "Telescope for Soft X-ray Astronomy, JGR 65, 773, 1960.

16. Vaiana, G. S., L. von Speybroeck, A. S. Krieger, J. K. Silk, A. Timothy, The S-054 X-ray Telescope Experiment on Skylab, Space Science Instrumentation 3,17-76, 1977.

17. Nolte, J. T. and E. C. Roelof, Corotation Between Chronospheric and Interplanetary Magnetic Field Polarities Near Solar Minimum, Solar Phys. 33, 241, 1973.

18. Snyder, C. W. and M. Neugebauer, 1966, R. J. Mackin and M. Neugebauer (eds.) Solar Wind, Pergamon Press, New York, 25-52.

19. Nolte, J. T., A. S. Krieger, C. V. Solodyna, Short-Term Evolution of Coronal Hole Boundaries, Solar Phys. 57, 129-139, 1978.

20. Bonetti, A., H. S. Bridge, A. J. Lazarus, E. F. Lyon, B. Rossi, and F. Scherb, Explorer X Plasma Measurements, Proceedings of Space Research III, the Third International Space Science Symposium, Washington, D. C., April 30-May 9, 1962, (ed. W. Priester) North-Holland Publishing Company, Amsterdam.

IX. Figures and Tables

Figure Captions

Figure 1 - Structure of the Corona above Coronal Holes

Figure 2 - Diagram of ATM X-ray Telescope

Figure 3 - Vel (km/sec) versus Carrington longitude during indicated Carrington rotation number.

Figures 4a, 6a, 8a, 10a, 12a - Vel (km/sec) versus Carrington longitude during indicated Carrington rotation number.

Figures 4b, 6b, 8b, 10b, 12b - Area (deg^2) versus time (days). The areas are the dark, light and total (= dark + light) areas within the hole and within a 20° x 20° window centered at the sub-earth point. Also marked are the interneg numbers used for each data point.

Figures 4c, 6c, 8c -Area (deg^2) versus time (days). The areas are the dark, light, and total areas within the hole and within a $\pm 10°$ band of latitudes. The interneg numbers used are also marked.

Figures 5a, 5b - Internegs of the 1604 crossing of CH1

Figure 7a - Internegs of the 1603 crossing of CH1

Figures 9a, 9b-Internegs of the 1602 crossing of CH1

Figure 10c - Area (deg^2) versus time (days). The areas are the dark, light and total areas within the hole and within a 10° x 10° window centered at the sub-earth point. Also marked are the interneg numbers used for each data point.

Figures 11a, 11b - Internegs of the 1607 crossing of CH2.

Figures 13a, 13b - Internegs of the 1606 crossing of CH2.

Tables

Fig.1

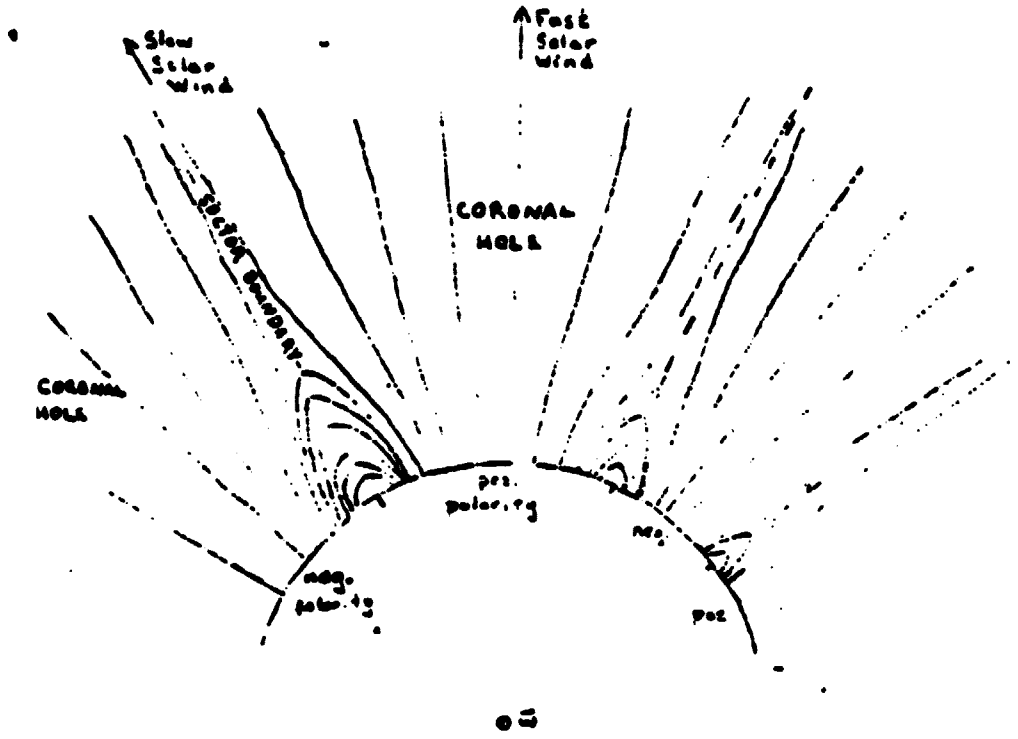

Fig.2

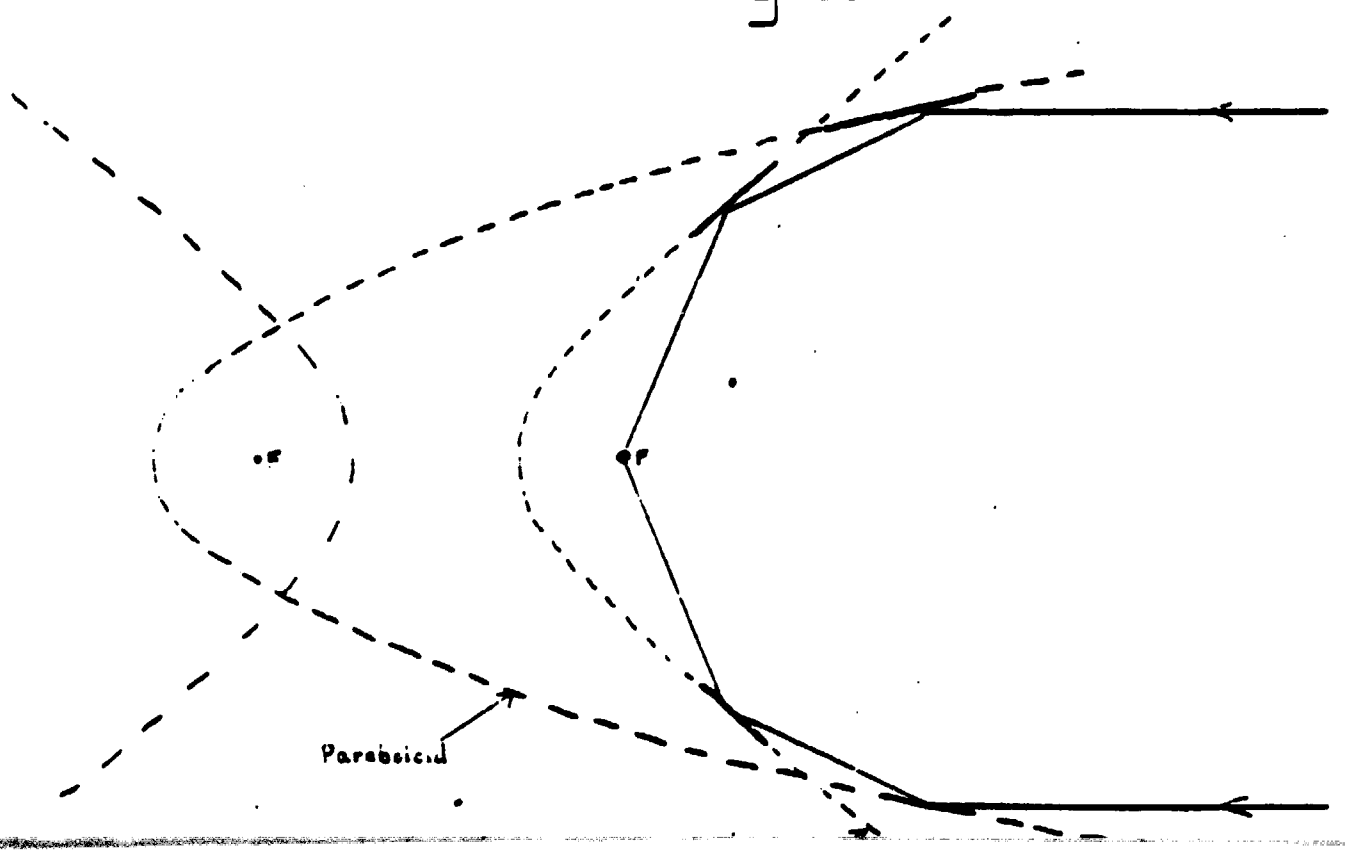

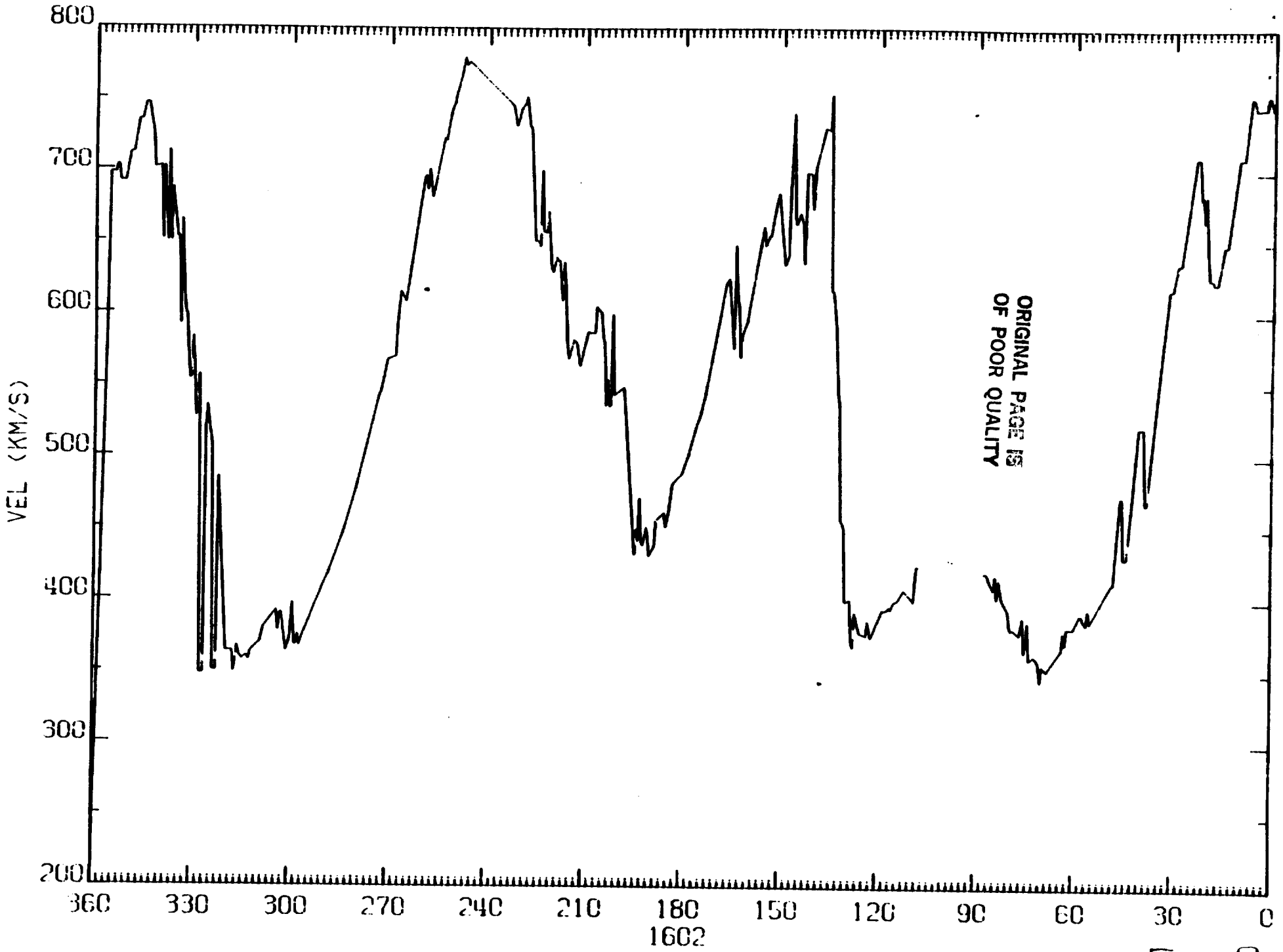
800
700
600
500
400
300
200
VEL (KM/S)
360
330
300
270
240
210
180
150
120
90
60
30
0
1602
ORIGINAL PAGE IS
OF POOR QUALITY

Fig. 3a

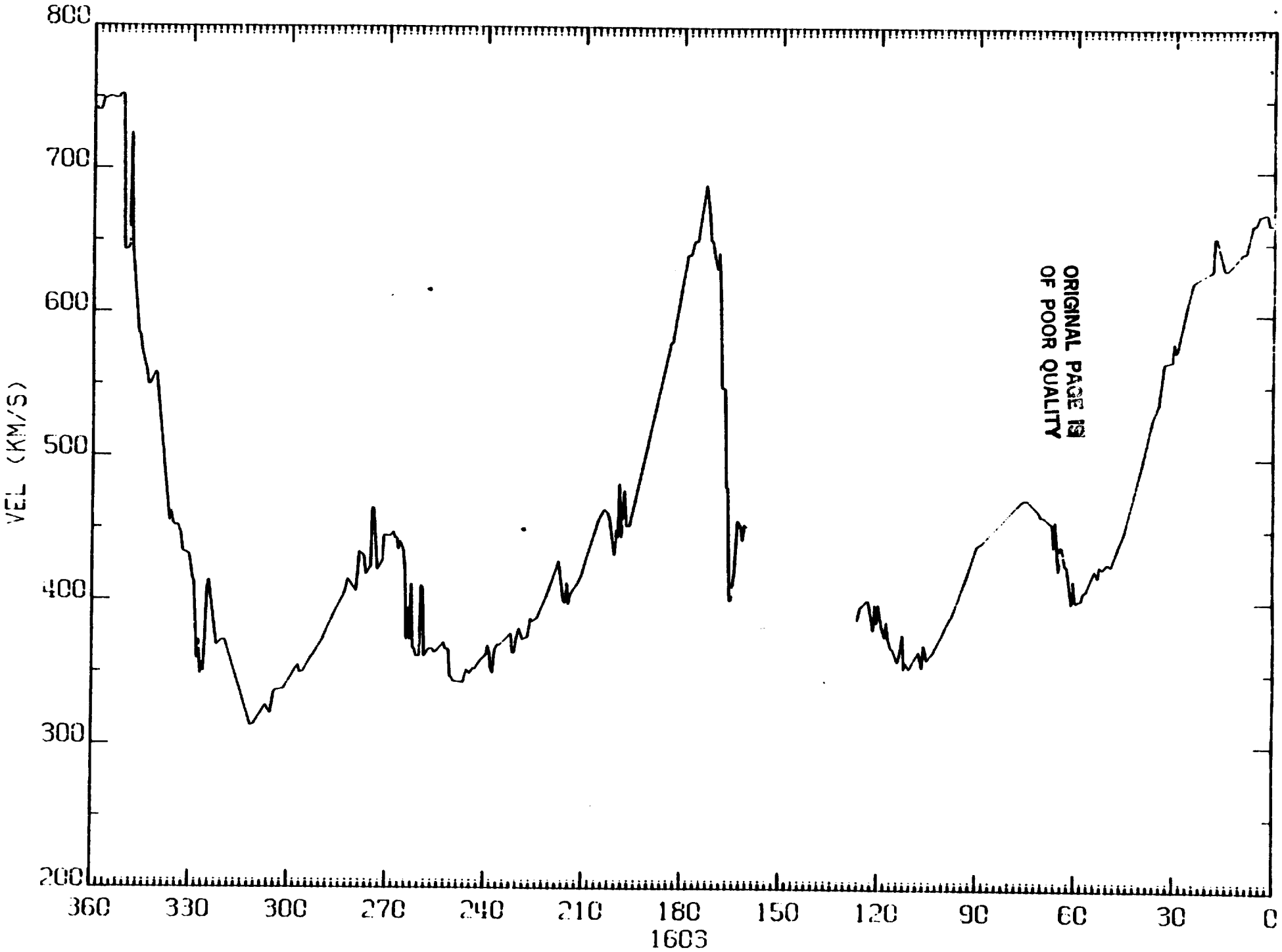
800
700
600
500
400
300
200
VEL (KM/S)
360
330
300
270
240
210
180
150
120
90
60
30
0
1603
ORIGINAL PAGE IS
OF POOR QUALITY

Fig. 3b

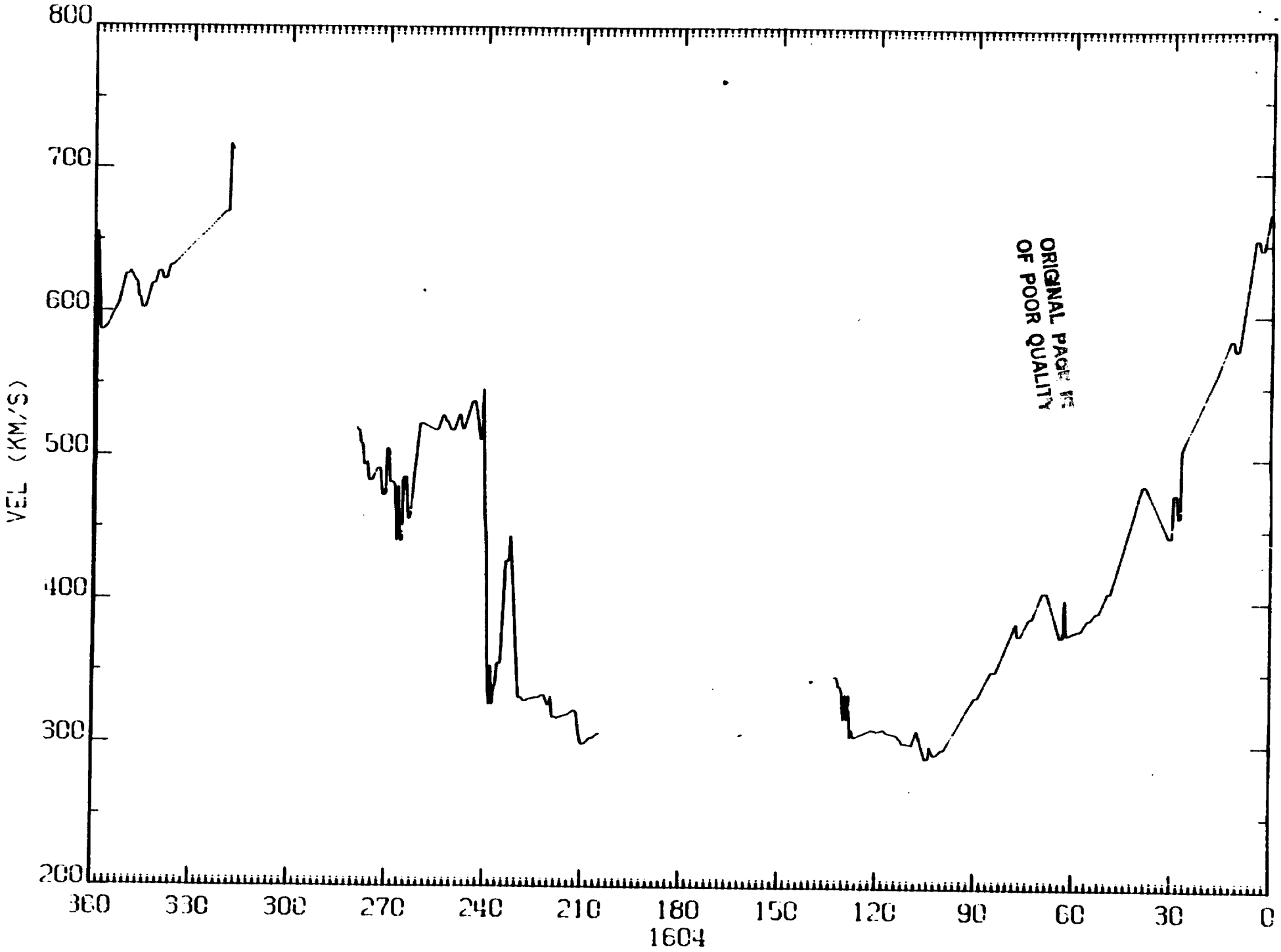

Fig. 3c

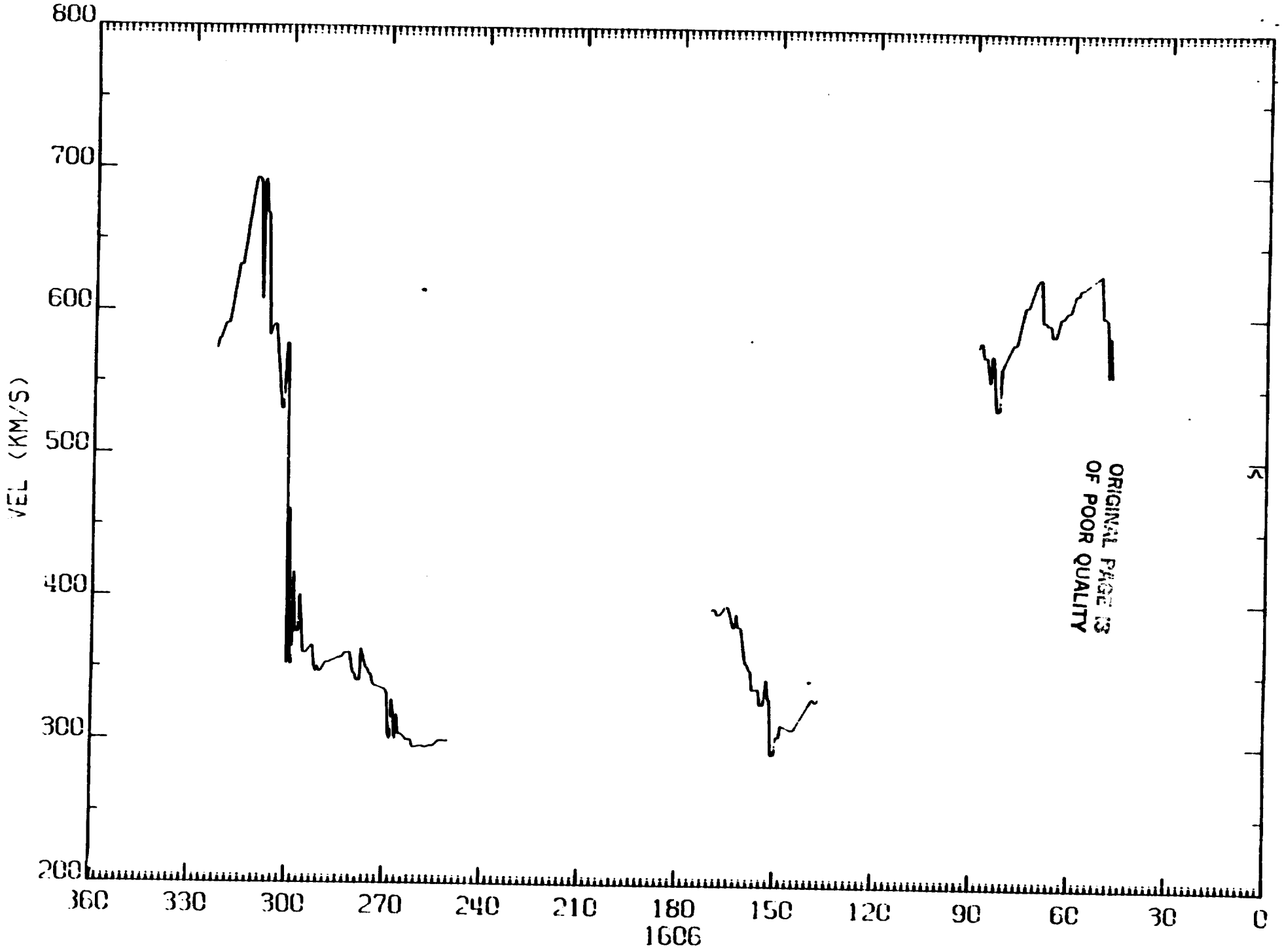
800
700
600
500
400
300
200
VEL (KM/S)
360
330
300
270
240
210
180
150
120
90
60
30
0
1606
ORIGINAL PAGE IS
OF POOR QUALITY

Fig. 3d

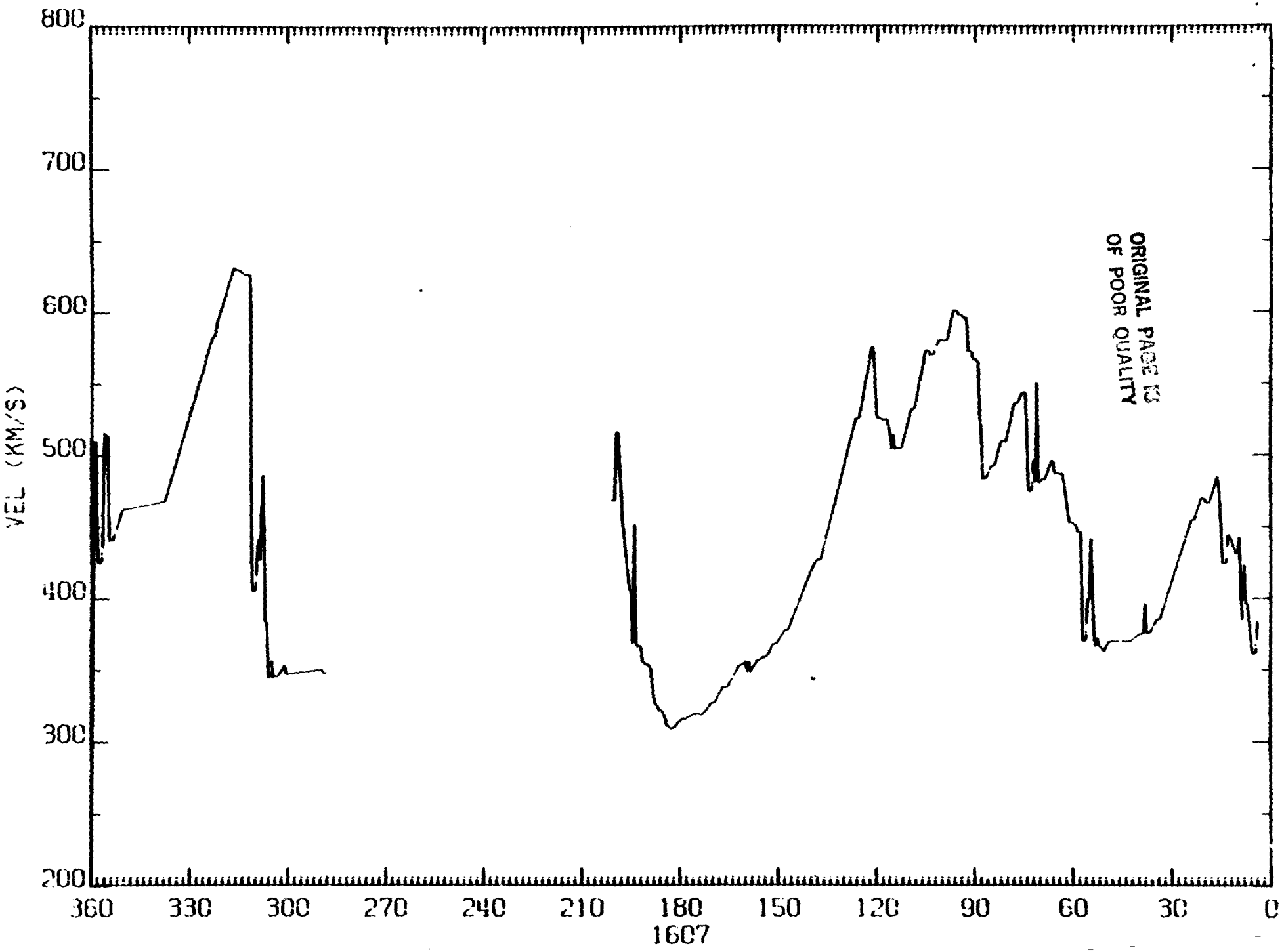
800
700
600
500
400
300
200
VEL (KM/S)
360
330
300
270
240
210
180
150
120
90
60
30
0
1607
ORIGINAL PAGE IS
OF POOR QUALITY

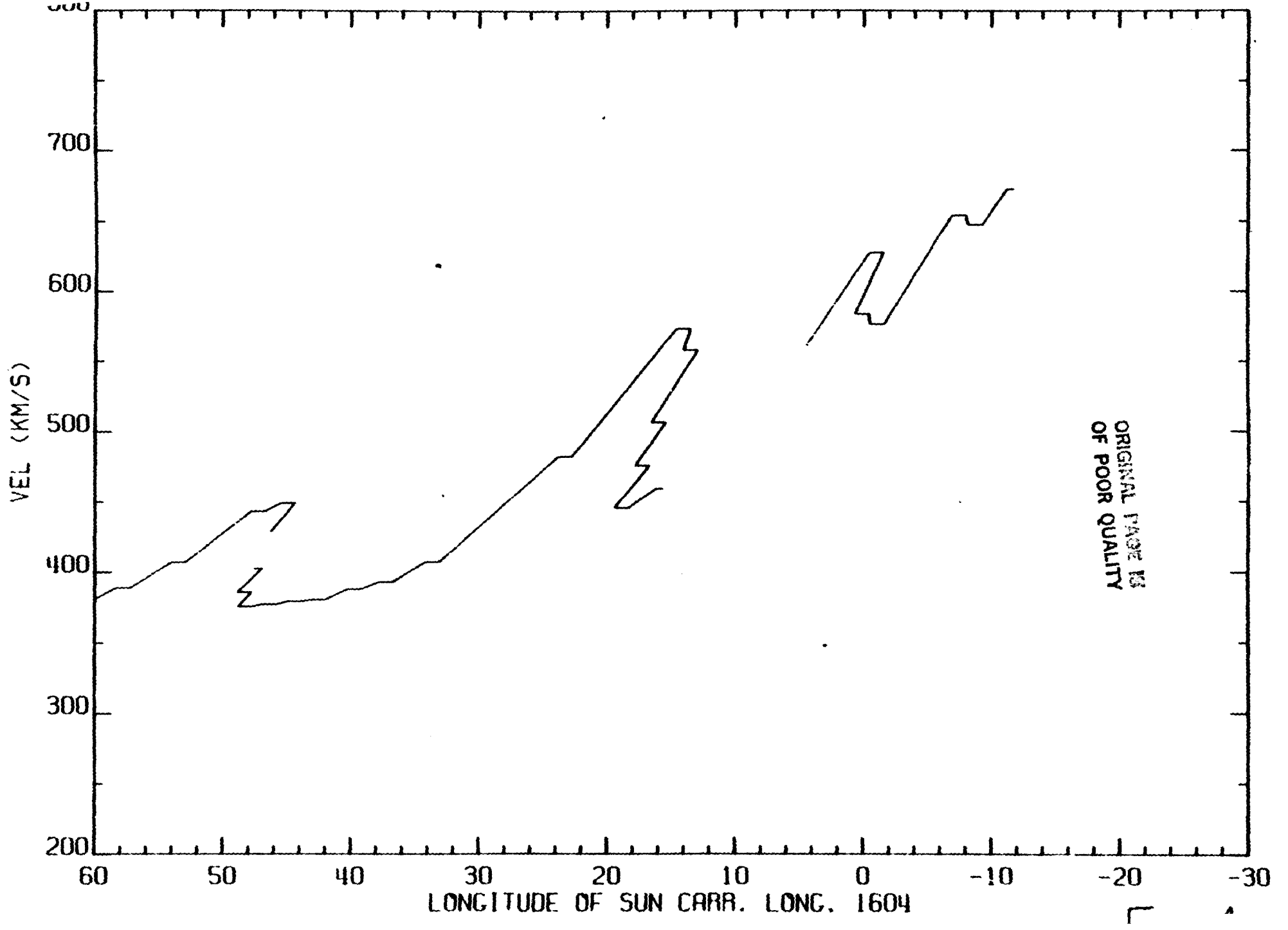

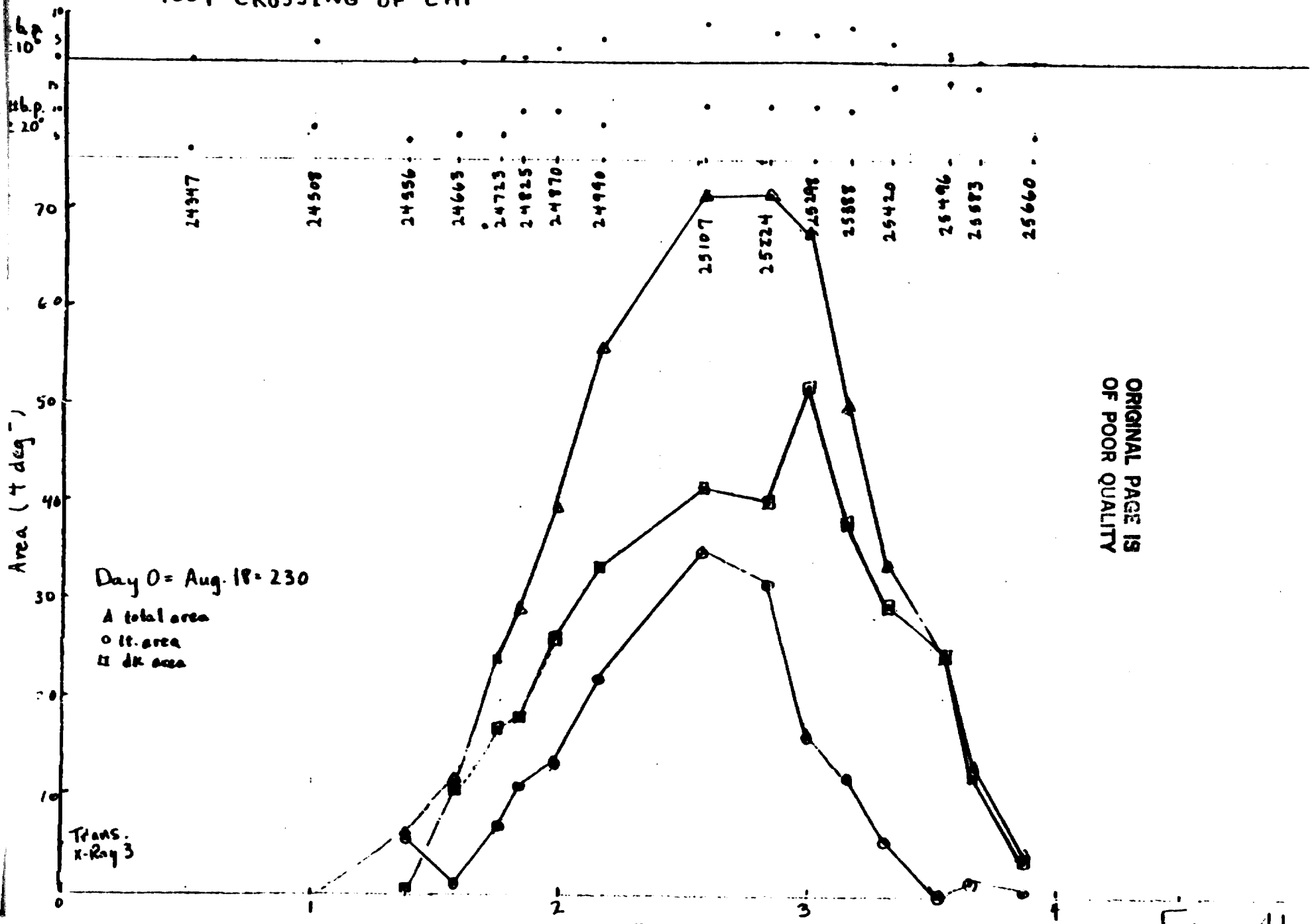
1604 CROSSING OF CHI
Area (4 deg⁻²)
Day 0 = Aug. 18 = 230
A total area
o lt. area
□ dk area
Trans. X-Ray 3
24347
24508
24956
24663
24713
24825
24870
24990
25107
25224
25288
25388
25420
25496
25583
25660
ORIGINAL PAGE IS OF POOR QUALITY

Fig. 41

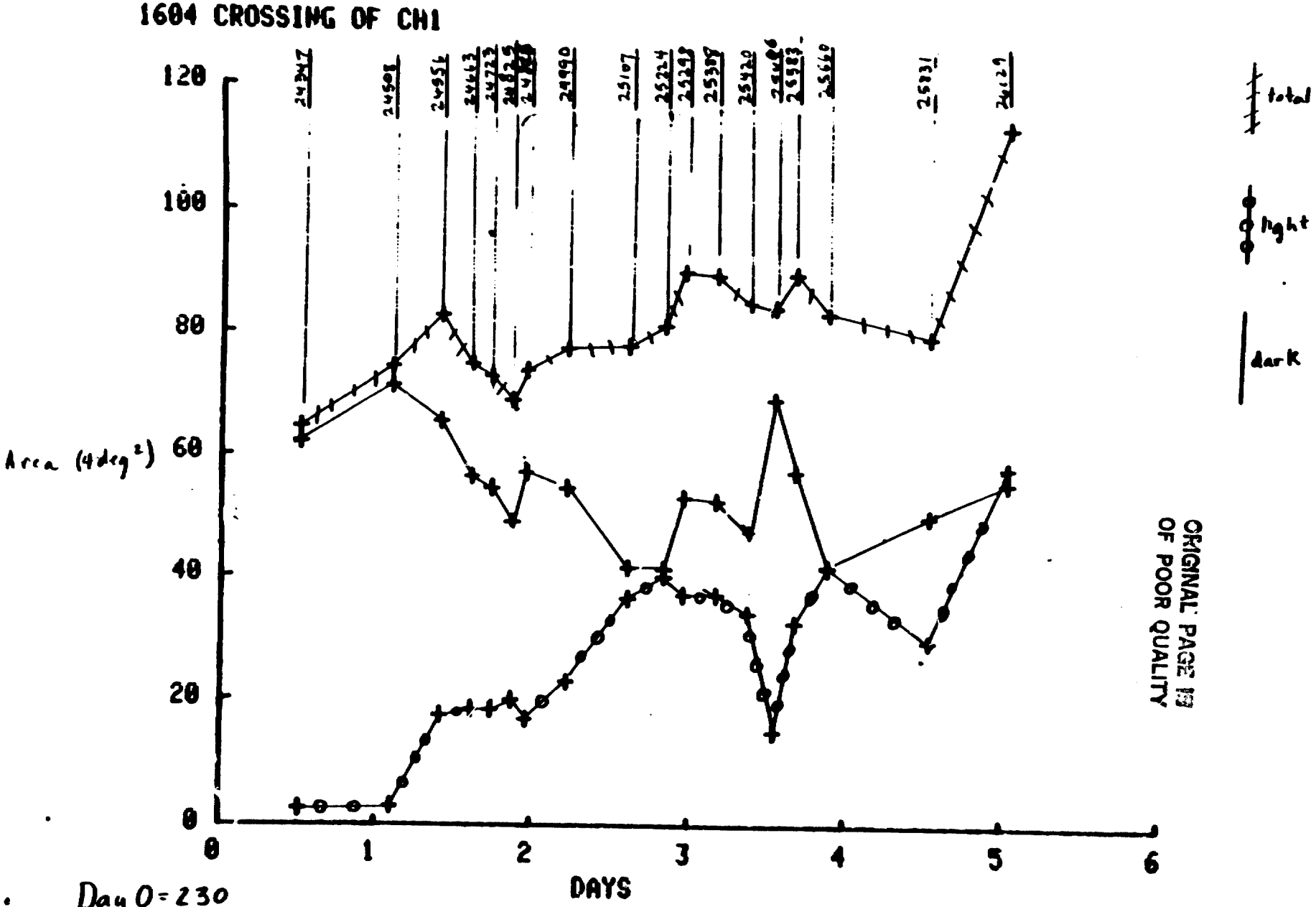

Fig. 4c

Fig. 54

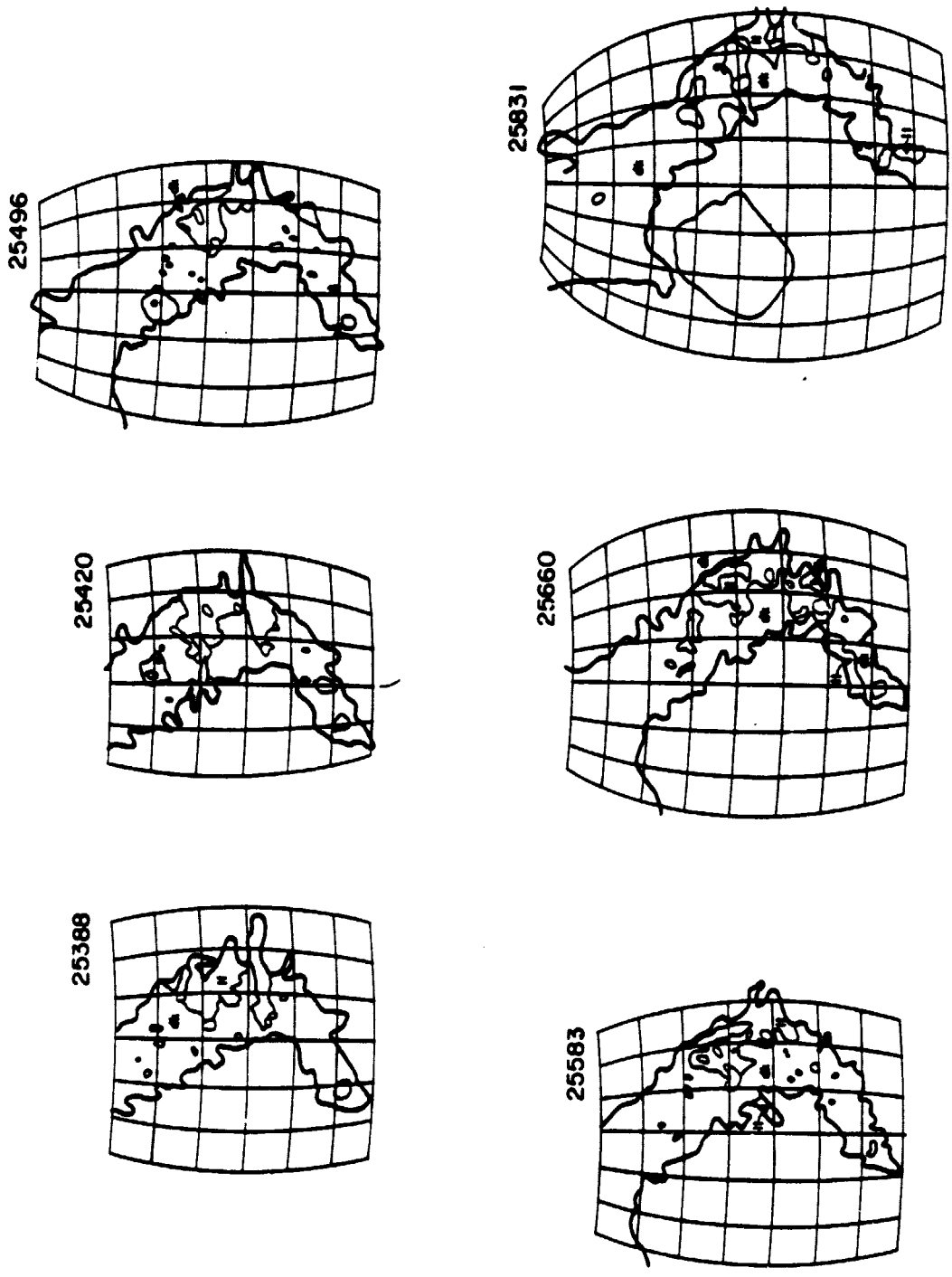

Fig. 56

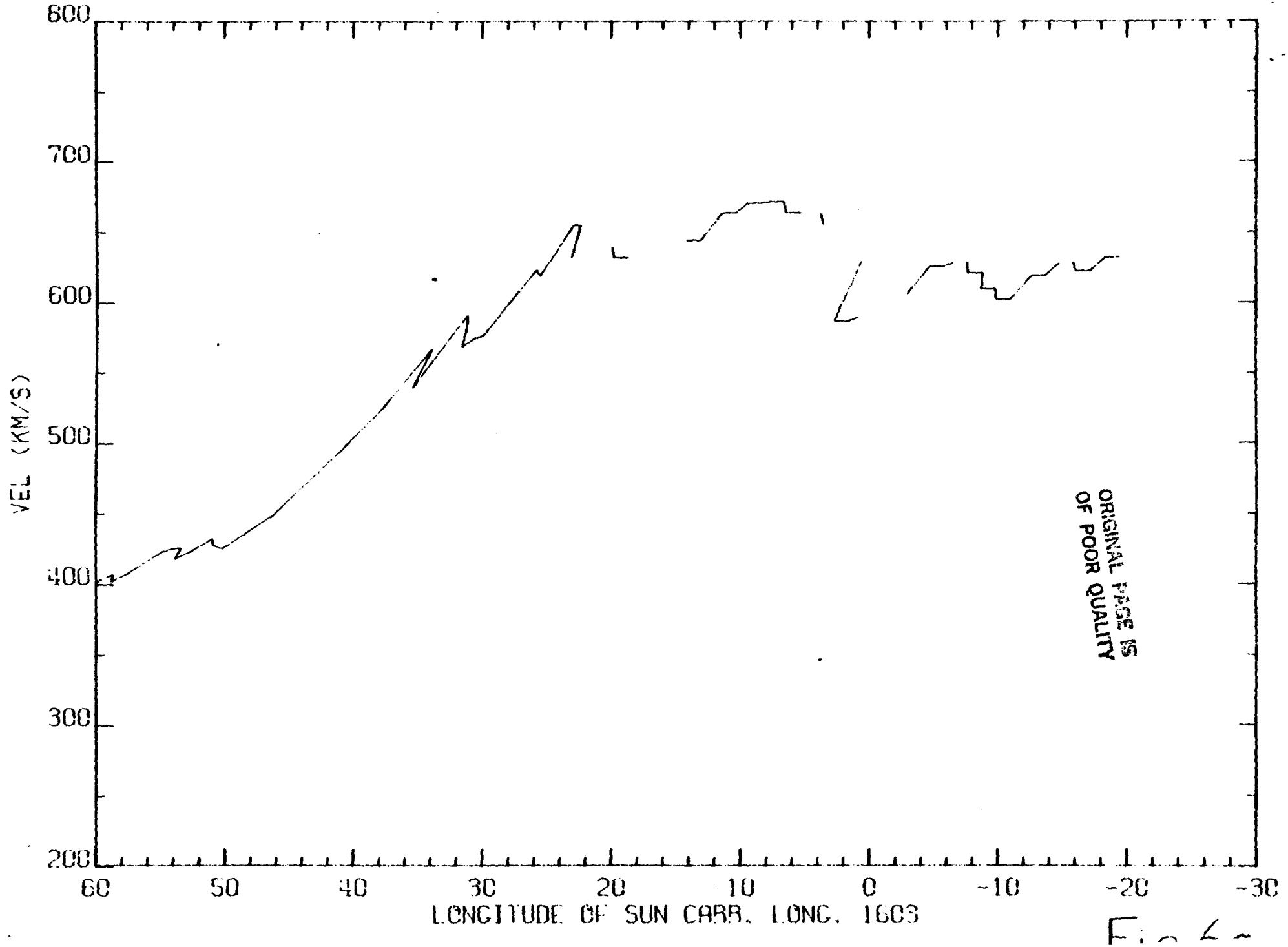

Fig 4a

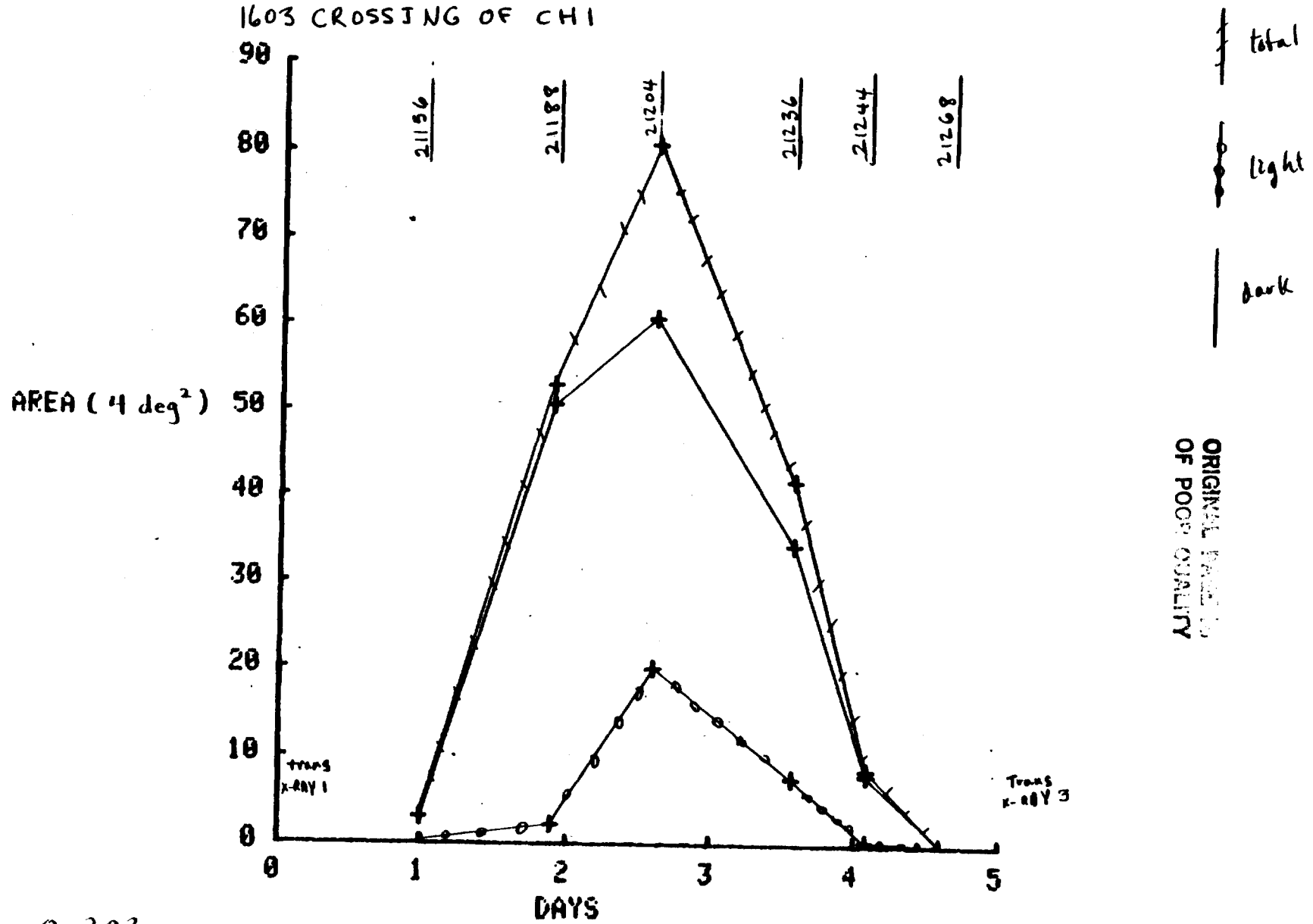

Day 0 = 203

Fig. 6b

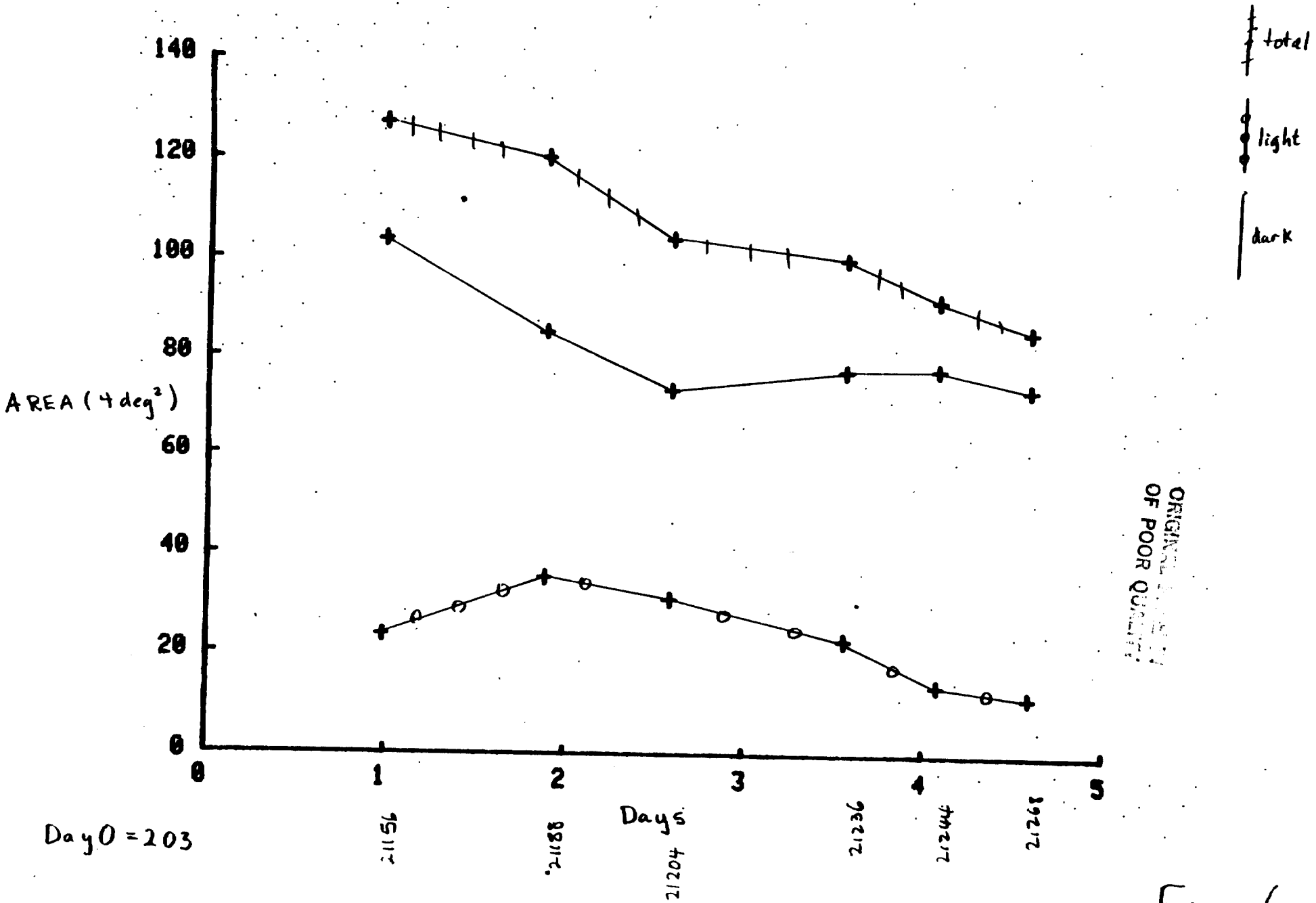

Fig. 6c

Fig 7L

Fig. 7b

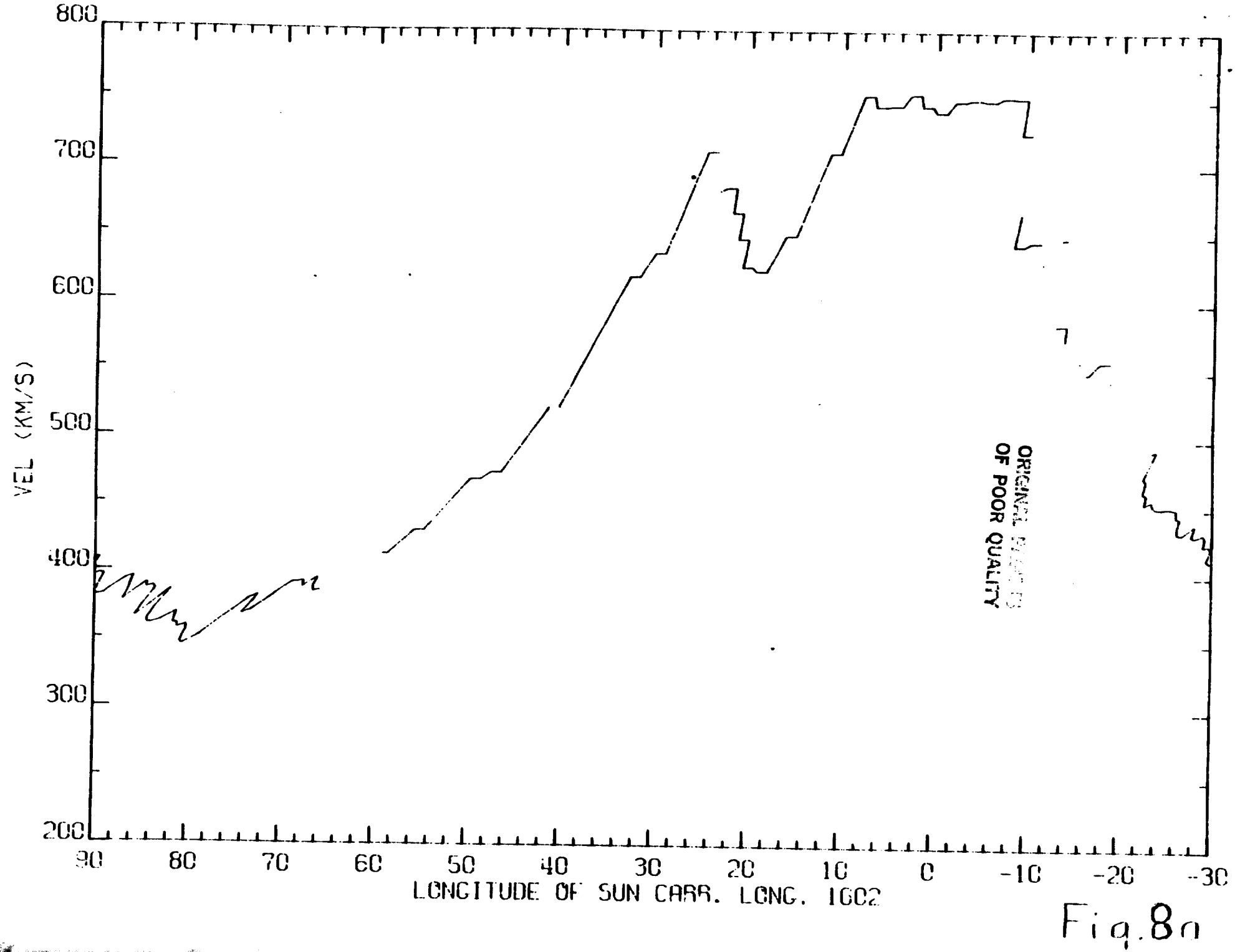
800
700
600
500
400
300
200
VEL (KM/S)
90
80
70
60
50
40
30
20
10
0
-10
-20
-30
LONGITUDE OF SUN CARR. LONG. 1002
ORIGINAL PAGE IS
OF POOR QUALITY

Fig.8a

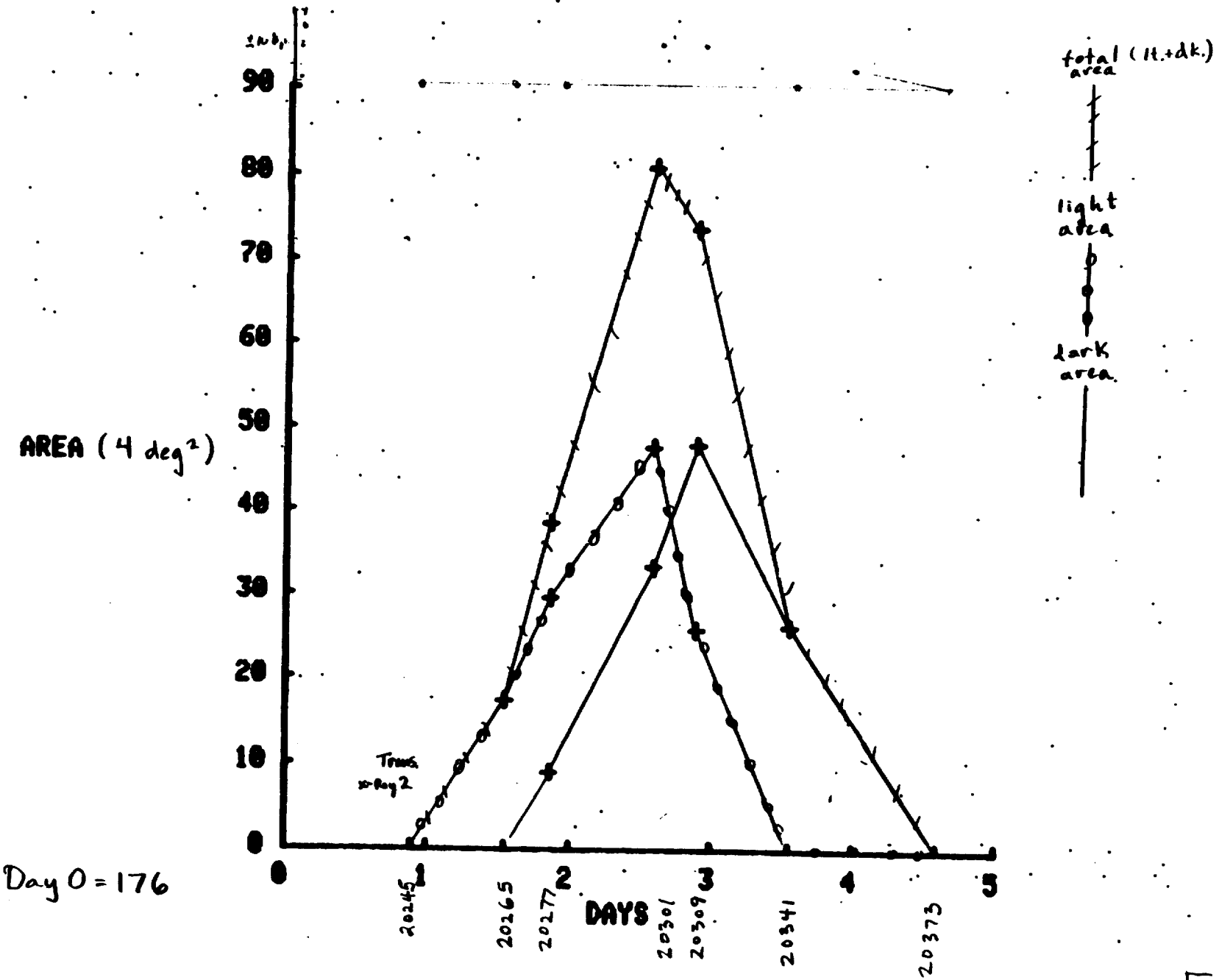

Fig. 8b

1602 CROSSING OF CH1

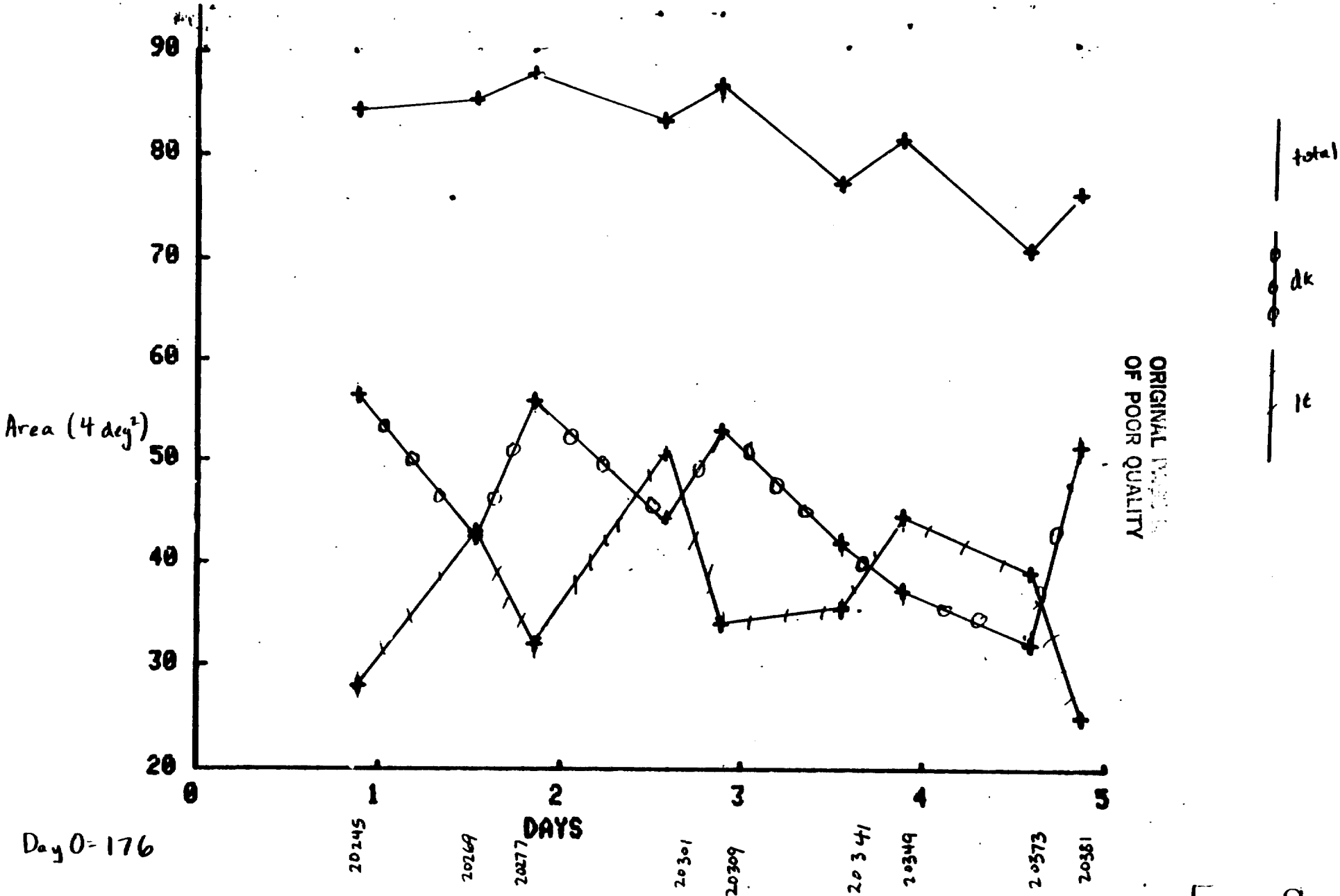

Day 0 = 176

Fig. 8c

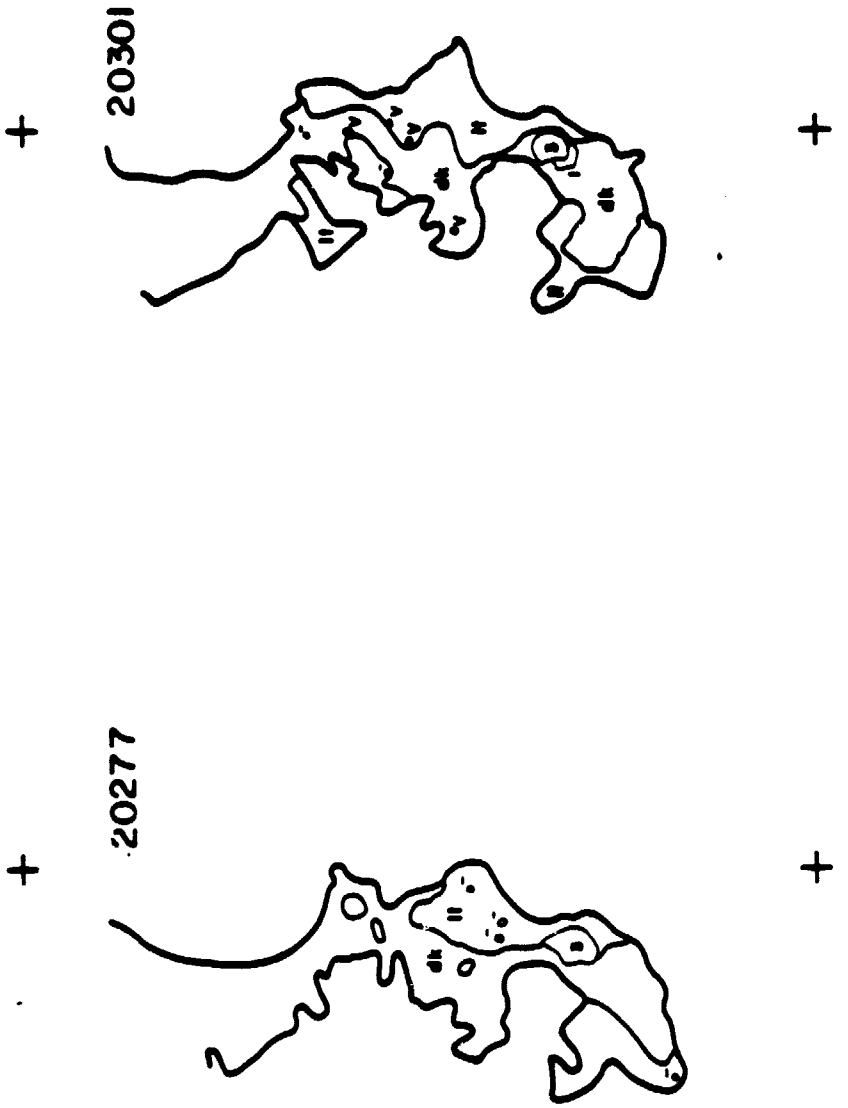

Fig. 9a

Fig. 96

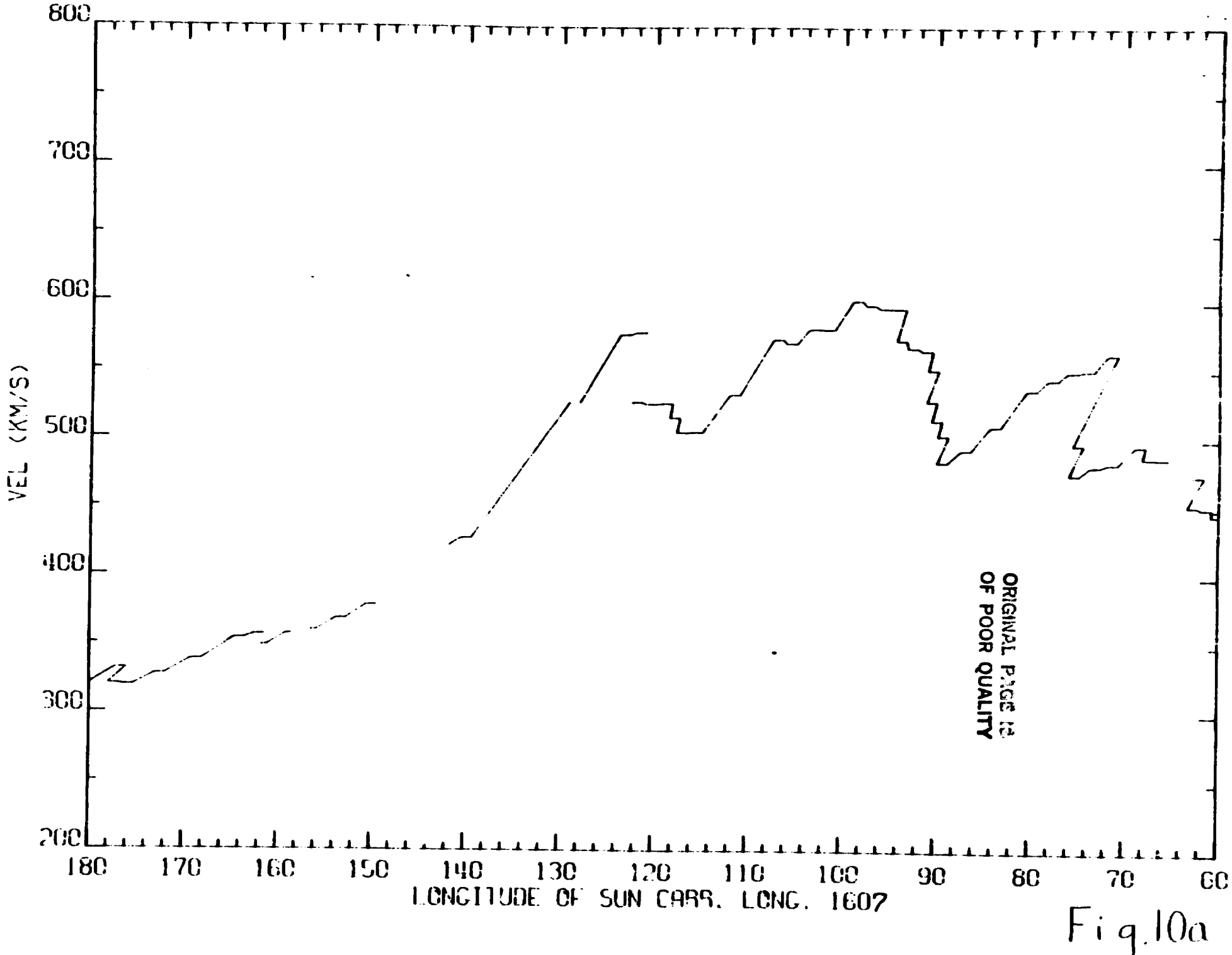
800
700
600
500
400
300
200
VEL (KM/S)
180
170
160
150
140
130
120
110
100
90
80
70
60
LONGITUDE OF SUN CARR. LONG. 1607
ORIGINAL PAGE IS
OF POOR QUALITY

Fig.10a

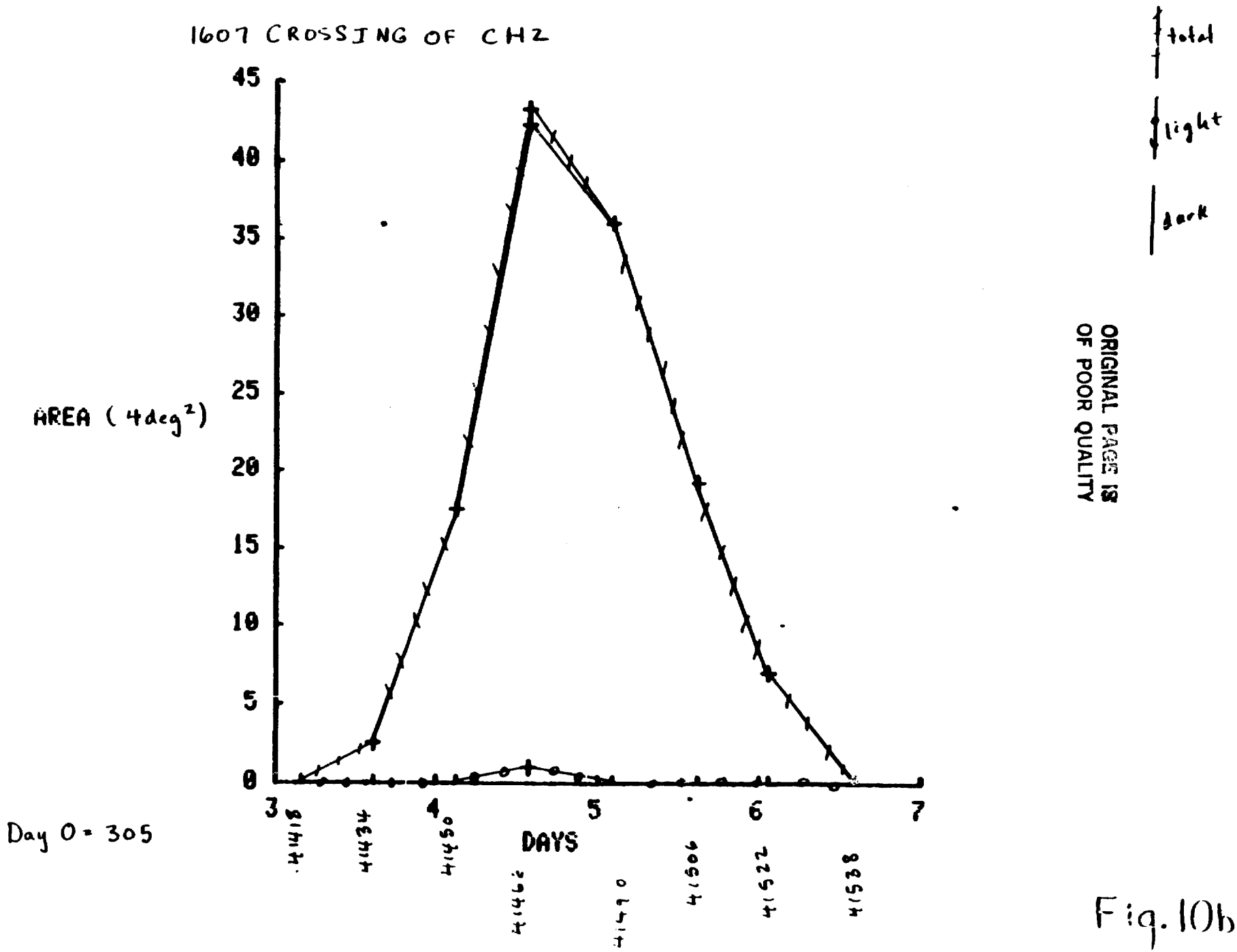

Fig. 10b

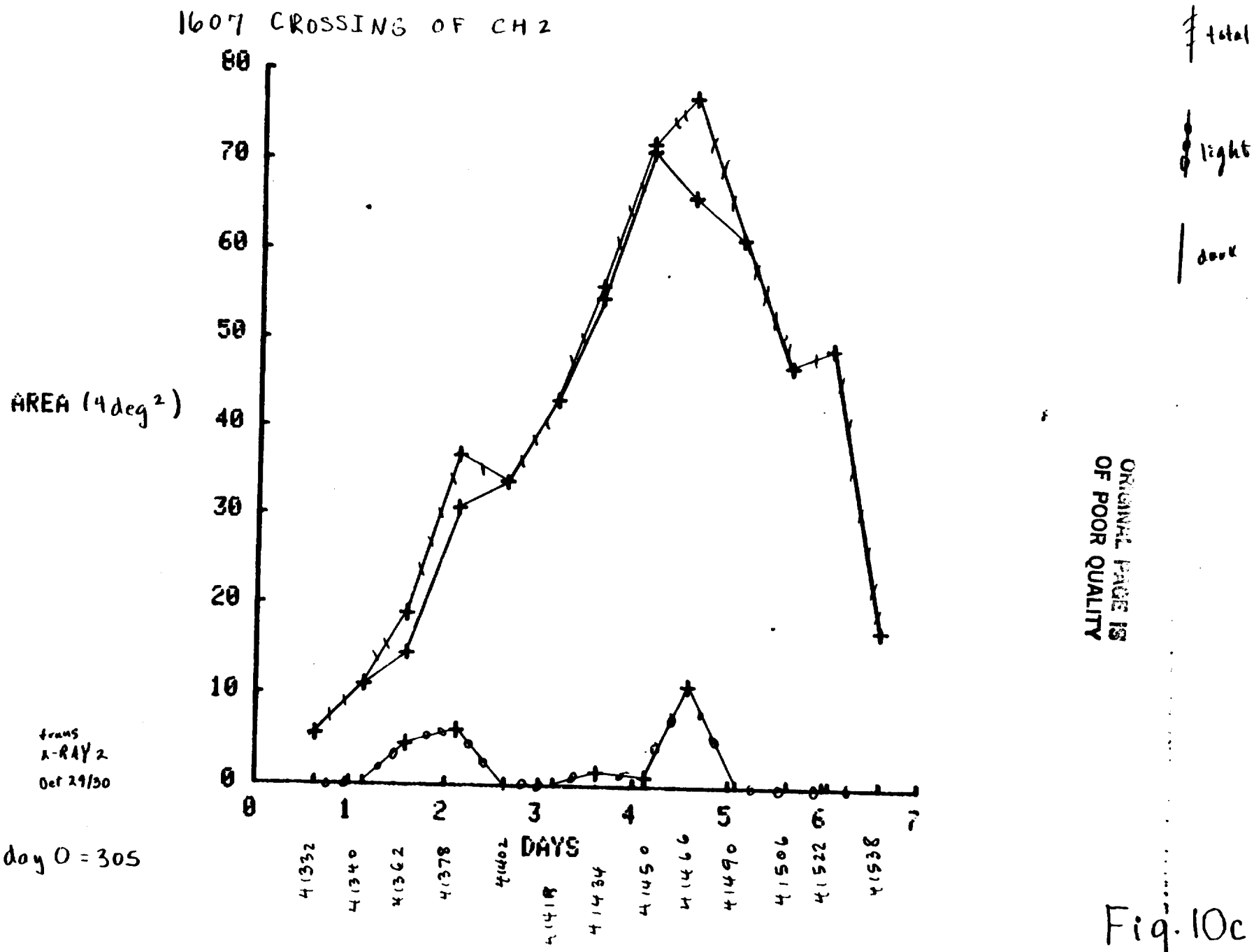

Fig. 10c

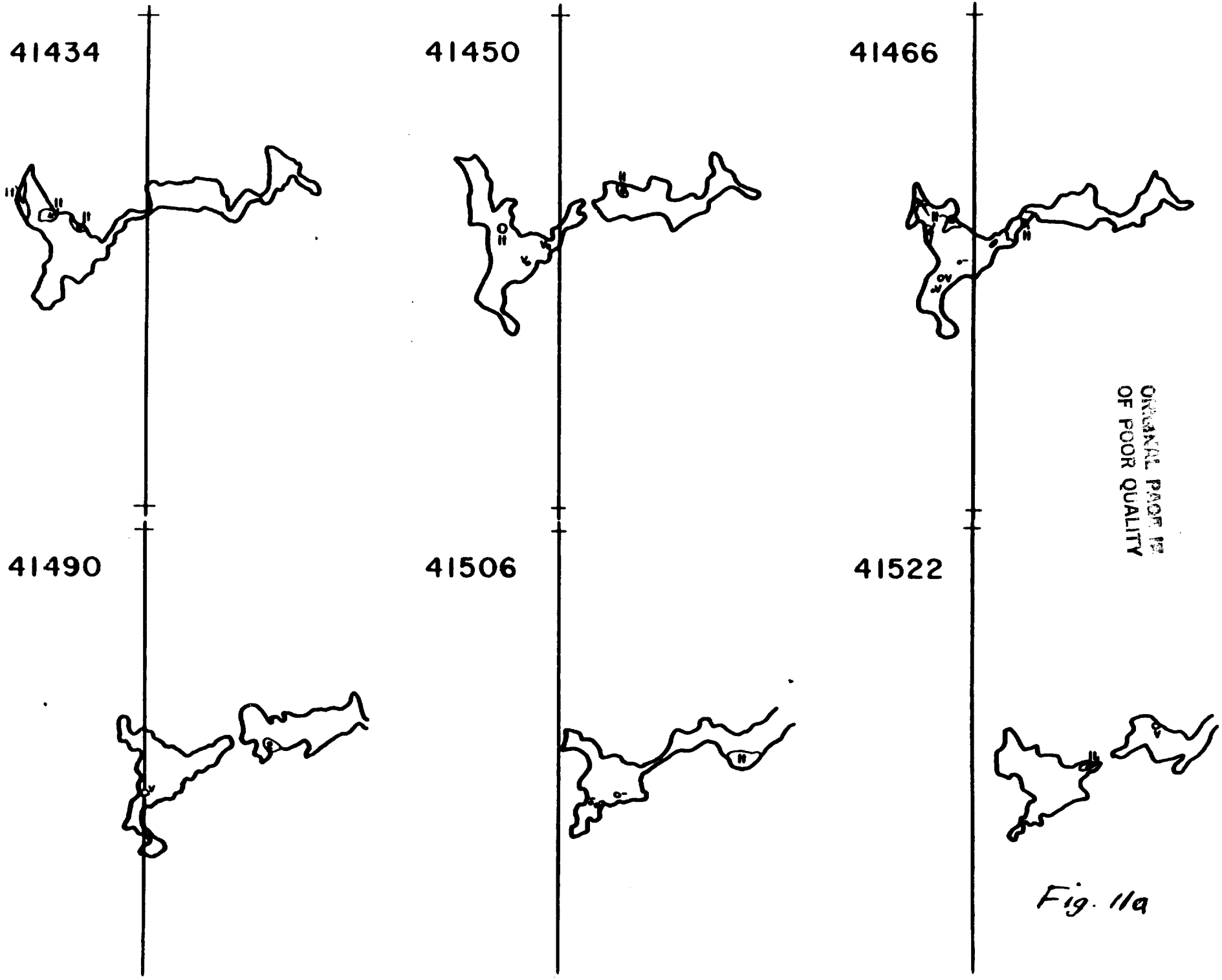

Fig. 11a

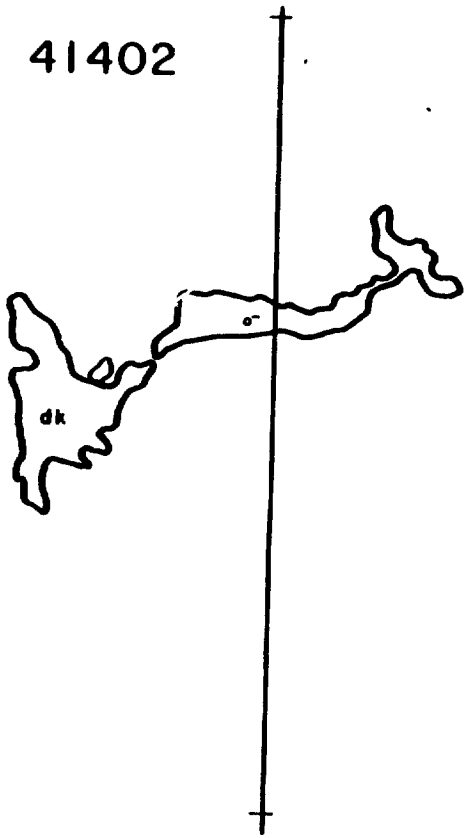

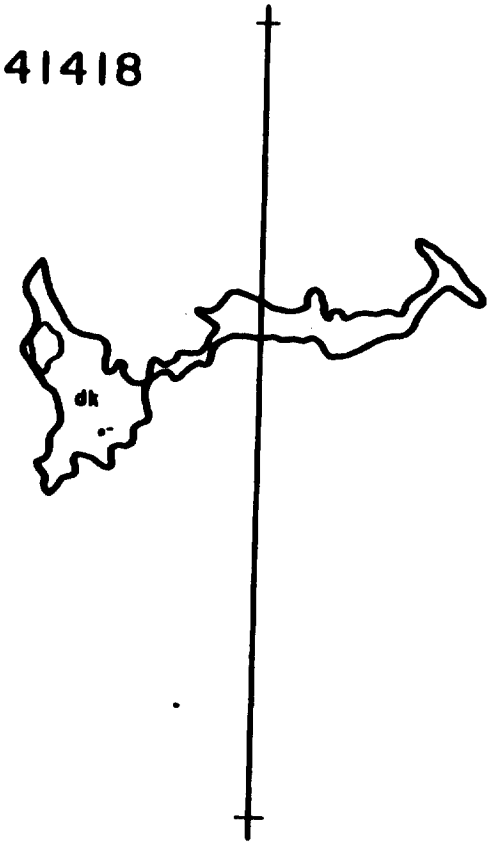

Fig. 116

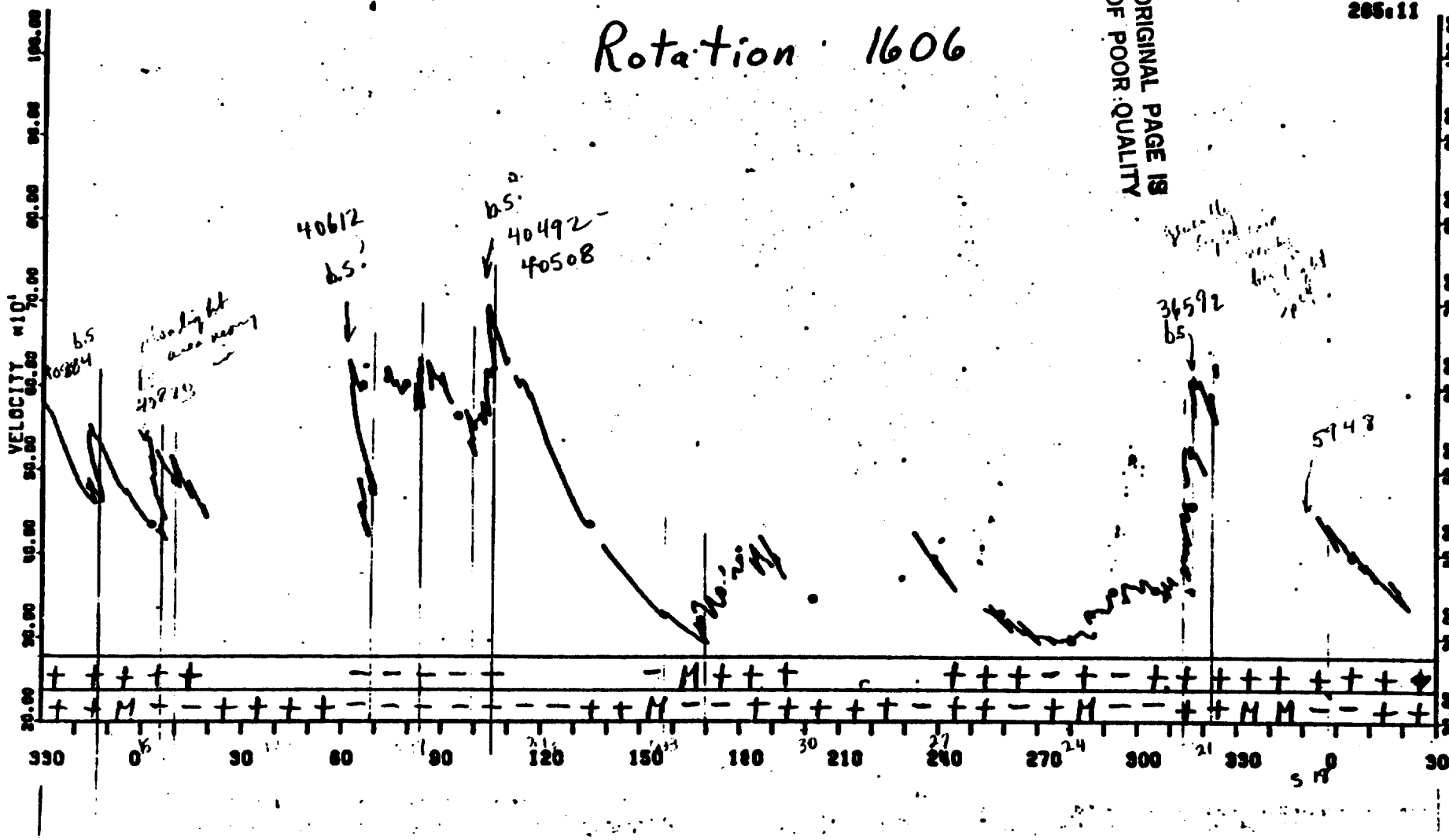
Rotation · 1606
ORIGINAL PAGE IS OF POOR QUALITY
285:11
VELOCITY ×10¹
40612
40492
40508
36592
5148
330
0
30
60
90
120
150
180
210
240
270
300
330
30

Fig. 12a

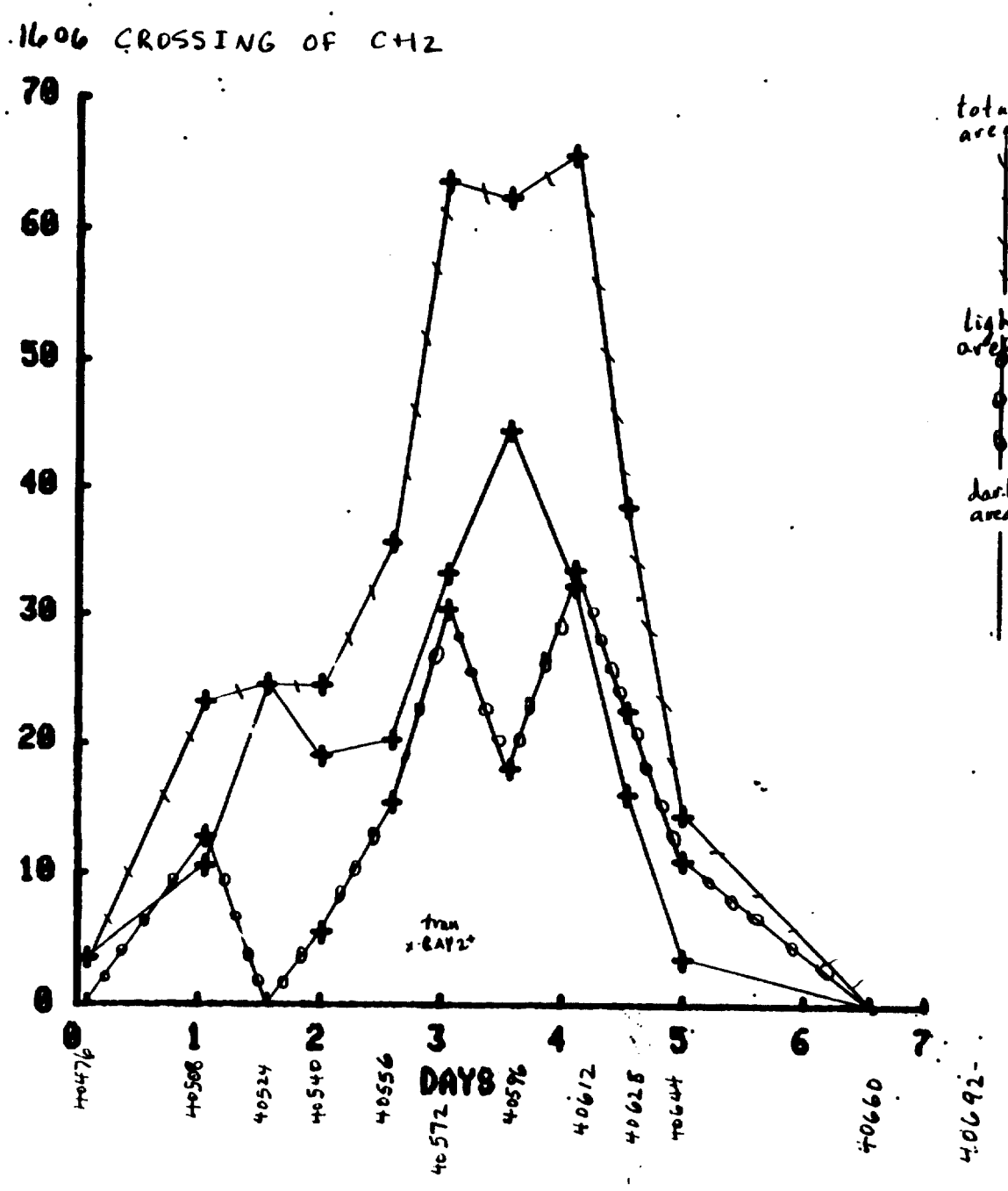

BREA

Day 0 = 279

ORIGINAL PAGE IS
OF POOR QUALITY

Fig. 17h

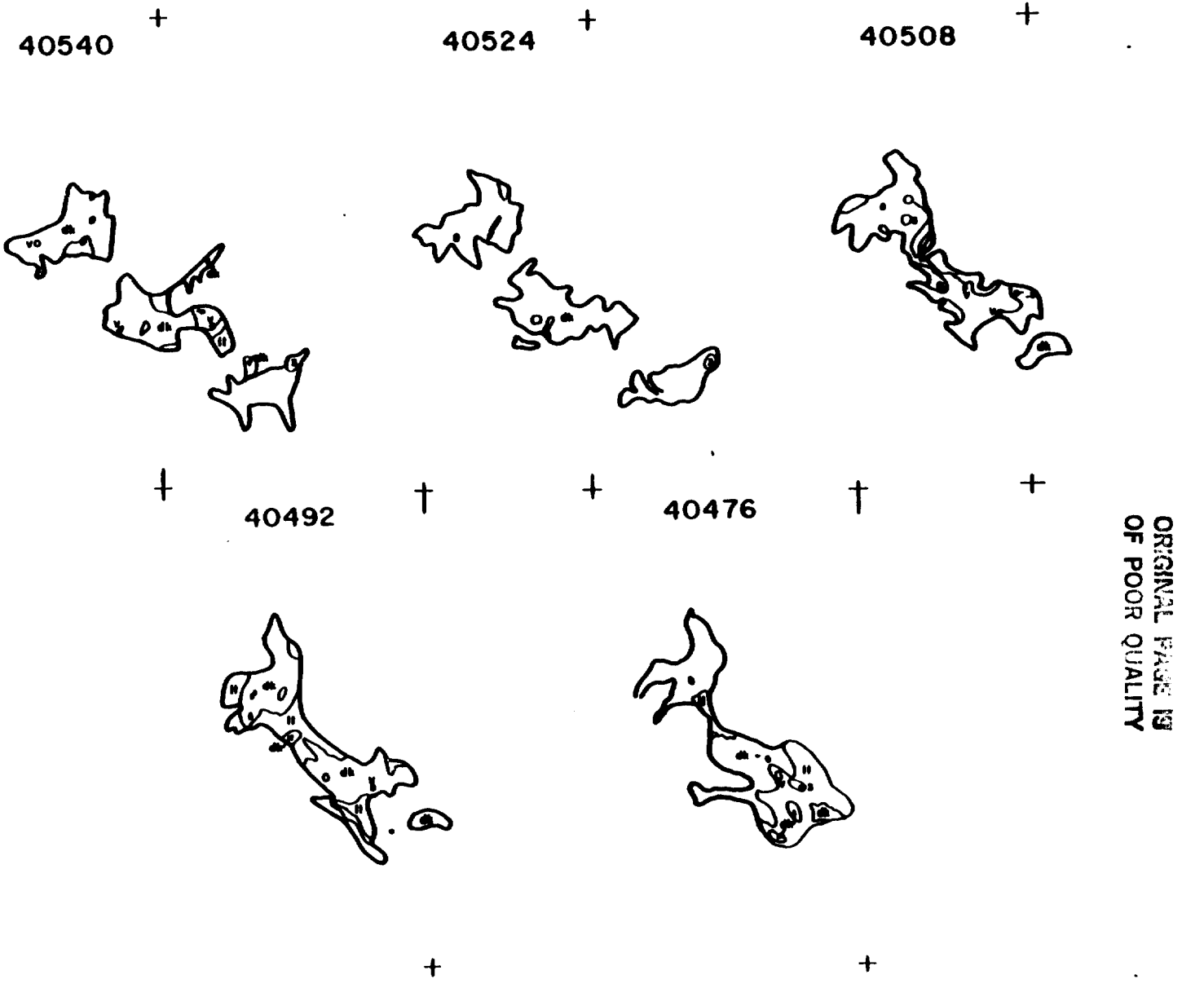

Fig. 13a

40596

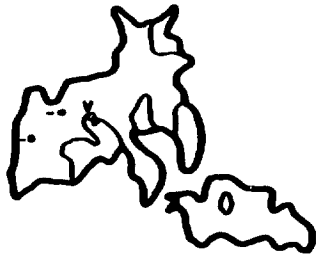

40572

40556

Fig. 136

Fig. 14

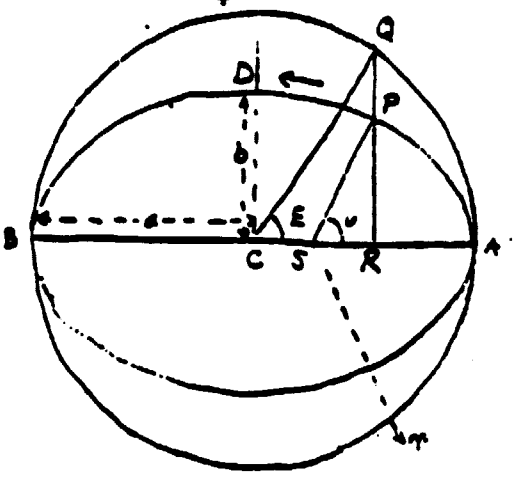

Fig. 15

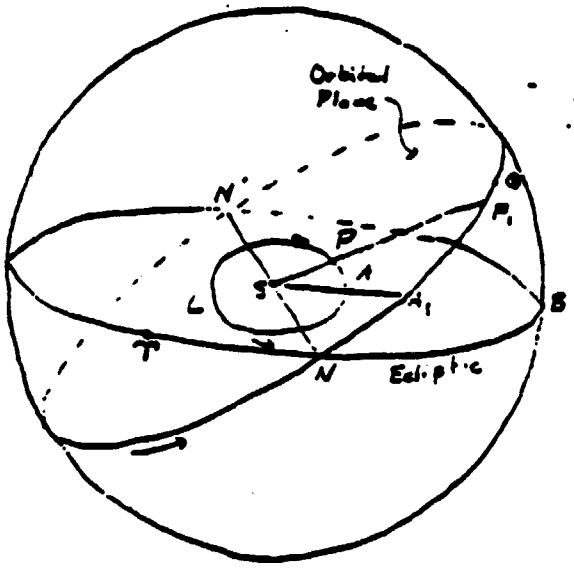

Fig. 16

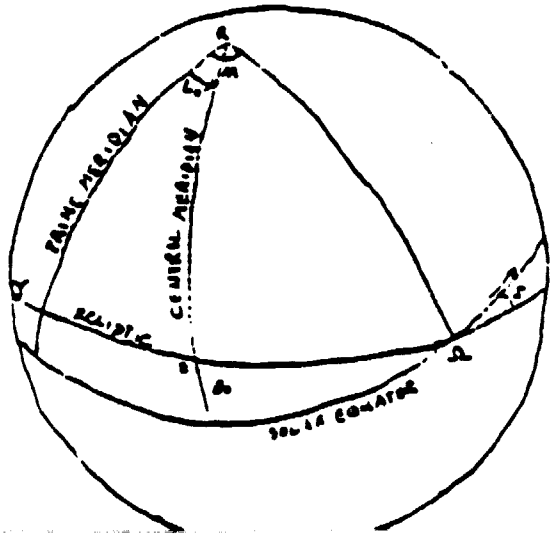

Table 1

ATM Telescope Filters

Filter Wheel Position No.	Material	Nominal Thickness (cm)	Measured Mass Thickness (mg/cm^2)	Pass Bands Å
1	Beryllium	1.3×10^{-3}	2.67	2-17
2	Teflon(CF_2)	3.2×10^{3}	0.62	2-14; 19-22
3	None			2-32; 44-54
4	Parylene -N**(C_8H_8)	5.7×10^{-4}	0.65	2-18; 44-47
5	Beryllium	5.1×10^{-3}	9.54	2-11
6	Beryllium	2.5×10^{-3}	4.72	2-14

Table 2: A List of Internegs Used In This Study

Interneg	Time (all in 1973)	Sub-earth Longitude (deg)
* 20245	176:21:17	40.2
20269	177:13:00	31.6
20277	177:20:33	27.4
20301	178:13:56	17.9
20309	178:21:25	13.8
20341	179:13:13	5.1
20349	179:21:26	0.6
20373	180:14:07	351.4
20381	180:20:46	347.7
* 21156	203:23:31	41.7
21188	204:21:21	29.7
21204	205:14:12	20.4
21236	206:13:20	7.63
21244	207:02:02	0.8
21268	207:14:07	354.0
24347	230:12:10	50.9
24508	231:02:24	43.1
24556	231:09:49	39.0
24663	231:14:36	36.4
24723	231:17:43	34.6
24825	231:20:48	32.9
24870	231:23:07	31.7
24990	232:05:09	28.3
25107	232:14:40	23.1
25224	232:20:03	20.1
25298	232:23:15	18.4
25388	233:04:23	15.5
25420	233:09:09	12.9
25496	233:13:09	10.7
25583	233:16:22	8.9
25660	233:21:14	6.3
25831	234:12:53	357.6
26120	[illegible]	[illegible]

Table 2 (continued)

Interneq	Time (all in 1973)	Sub-earth Longitude (deg)
* 40476	279:02:00	129.5
40492	279:14:16	122.7
40508	280:01:14	116.7
40524	280:13:32	110.0
40540	281:00:32	103.9
40556	281:14:16	96.4
40572	282:01:25	90.2
40596	282:13:42	83.5
40612	283:02:35	76.3
40628	283:13:06	70.5
40644	284:00:01	64.6
40660	284:14:09	56.8
40692	285:13:11	44.1
* 41332	305:15:02	139.3
41340	306:03:25	132.6
41362	306:14:12	126.7
41378	307:02:55	119.7
41402	307:15:06	112.9
41418	308:03:50	106.0
41434	308:14:24	100.0
41450	309:02:50	93.3
41466	309:13:37	87.3
41490	310:02:12	80.5
41506	310:14:58	73.5
41522	311:01:27	67.6
41538	311:14:20	60.5

*Finest time resolution available was used.

Table 3: X-Ray Transients Within ±15° of G.M.P.

Date	LOPE	First Vis	Lat	Long	X-Ray Imp.	AR non-AR	Est Prob. Onset Time
25/26 June	2116	1259	S13	W13	2	AR	1245-1259
20/21 July	1343	0059	S30	CM	3	N	20,1343-1900
21/22 July	1314	0015	N35	E16	1	N	21,1715-2215
27 July	0257	1507	S25-40	E50-10	3	N	27,0430-0530
18 August	2131	2255	S40-50	E05-W40	3	N	18,2140-2145
24 August	0024	2347	S05	CM	2	N	
8/9 October	1415	0123	S20	W15	2+	N	8,1745-2240

```
0001          SUBROUTINE CARRBL (NYR,$DAY,BSE,XLSE,NCARR,DIST)
              C  THIS RETURNS THE CARRINGTON LONGITUDE(XLSE), LONGITUDE(BSE) OF THE SUB EARTH
              C  POINT.  IT ALSO RETURNS THE CARRINGTON ROTATION NUMBER AND EARTH SUN DISTANCE
              C  ONE SUPPLIES THE YEAR AND DOUBLE PRECISION DAY OF THE YEAR
0002          IMPLICIT REAL*8($)
              C  $JULDB IS THE JULIAN DAY NUMBER AND IS THE ELAPSED NUMBER OF DAYS SINCE
              C  JULIAN DAY = 0 = JAN. 1, 4713 B.C. AT GREENWICH MEAN NOON
0003          $JULDB=365.*(NYR-1)+(NYR-1)/4-(NYR-1)/100.+(NYR-1)/400
             1 +$DAY+1721425.500
              C  JULIAN DAY 2415020.0 IS THE START OF THE EPOCH OF 1900
0004          $D = $JULDB-2415020.000
0005          $D2 = $D*$D
0006          $D3 = $D2*$D
              C  $OMEGA IS THE HELIOGRAPHIC LONGITUDE OF THE ASCENDING NODE OF THE SOLAR
              C  EQUATOR ON THE ECLIPTIC
0007          $OMEGA = 1.28572590D+2.437D-4*(NYR-1850)
              C  $AN IS THE HEL. LONG. OF THE NODE OF THE EQUATOR
0008          $AN = 360.0D0-360.0D0/25.38D0*($JULDB-2398220.0D0)
0009          $AN = DMOD($AN,360.0D0)
0010          $AN = $AN*0.01745329D0
              C  $EMM IS THE MEAN ANOMALY OF THE SUN IN GEOCENTRIC COORDS,
0011          $EMM = 358.4758444D0+0.985600267D0*$D-1.12D-13*$D2-6.0D-20*$D3
0012          $EMM = DMOD($EMM+360.0D0,360.0D0)
0013          $EMM = $EMM*0.01745329D0
              C  $OMB IS THE LONGITUDE OF PERIHELION FROM THE MEAN EQUINOX OF DATE IN GEOCENT-
              C  RIC COORDS. OF THE SUN
0014          $OMB = 281.2208333D0+4.706850D-5*$D+3.39D-13*$D2+6.0D-20*$D3
0015          $OMB = DMOD($OMB+360.0D0,360.0D0)
0016          $OMB = $OMB*0.01745329D0
              C  $ECC IS THE ECCENTRICITY OF THE SUNS ORBIT
0017          $ECC = 0.01675101D0-1.1444D-9*$D-9.4D-17*$D2
              C  $ECA IS THE ECCENTRIC ANOMALY, THE NEXT STEPS UNTIL 100 CALCULATE THE
              C  ECCENTIC ANOMALY FROM THE MEAN ANOMALY AND THE ECCENTRICITY
0018          $ECA = $EMM
0019          DO 100 I=1,5
0020          $ECA = $EMM+$ECC*DSIN($ECA)
0021      100 CONTINUE
              C  DIST IS THE EARTH SUN DISTANCE IN ASTRONOMICAL UNITS
              C  DIST IS THE EARTH SUN DISTANCE IN UNITS OF THE SEMI-MAJOR AXIS OF THE ORBITAL
              C  ELLIPSE WHICH IS THE ASTRONOMICAL UNIT
0022          DIST = 1.0D0-$ECC*DCOS($ECA)
              C  $VEE IS THE TRUE ANOMALY OF THE SUN IN GEOCENTRIC COORDS.
0023          $VEE = 2.0D0*DATAN(DSQRT((1+$ECC)/(1-$ECC))*DTAN($ECA/2.0D0))
0024          IF (DABS($VEE-$ECA).GE.1.570796D0)$VEE=$VEE+3.14159265300
0025          IF (DABS($VEE-$ECA).GE.1.570796D0)$VEE=$VEE+3.14159265300
              C  $ELL IS THE TRUE LONG. OF THE SUN IN GEOCENTRIC ECLIPTIC COORDINATES
0026          $ELL = $VEE+$OMB
0027          $ELL = DMOD($ELL,6.28318530700)
              C  $BSE IS THE LATITUDE OF THE SUB-EARTH POINT IN HELIOGRAPHIC COORDINATES
0028          $BSE = DARSIN(DSIN($ELL-$OMEGA)*0.126200)
0029          $BSE = $BSE*57.29577951D0
              C  $ELLSE IS THE LONG. OF THE SUB-EARTH POINT IN HELIOGRAPHIC COORDINATES.
              C  THE QUADRANT OF ($ELL-$OMEGA) IS THE QUADRANT OF ($ELLSE-$AN)+0R-180
```

```
0030                    $ELLSB = DATAN(DTAN($ELL-$OMEGA)*0.992D0)
0031                    $ELLSB = DMOD($ELLSB+6.283185307D0,6.283185307D0)
0032                    $DIF=DMOD($ELL-$OMEGA+6.283185307D0,6.283185307D0)
0033                    $DIF = DABS($ELLSB-$DIF)
0034                    IF ($DIF .LT. 1.57079632D0 .OR. $DIF .GT. 4.712388981D0)
                       Y$ELLSB = $ELLSB+3.141592653D0
0035                    $ELLSE = $ELLSB+$MN
0036                    $ELLSE = $ELLSE*57.2957795100
0037                    $ELLSE = DMOD($ELLSE+360.000,360.000)
                C  FOLLOWING IS CALCULATED THE CARRINGTON ROTATION NUMBER.  THE CARRINGTON
                C  SIDEREAL PERIOD IS NOT EXACTLY CONSTANT
0038                    $NCARR =  ($JULDB-2398140.1070D0)/27.2753D0
0039                    IF($ELLSE .LE. 25.0D0 .AND. $ELLSE .GE.0.000) $NCARR=($JULDB-
                       12398143.1070D0)/27.2753D0
0040                    IF($ELLSE .LE. 360D0 .AND. $ELLSE .GE. 335.000) $NCARR=
                       1($JULDB-2398137.1070D0)/27.2753D0
0041                    NCARR = $NCARR
0042                    XLSE = $ELLSE
0043                    BSE = $BSE
0044                    RETURN
0045                    END
```

REVISED

INTRA-STREAM STRUCTURE OF SOLAR WIND

ERIC R. ASLAKSON
James D. Sullivan (both at: Center for Space Research and Department of Physics, M.I.T., Cambridge, MA 02139)
David F. Webb, American Science & Engineering, Arlington, MA 02174)

Changes of features in coronal holes observed from American Science & Engineering's (AS&E) x-ray telescope pictures were examined to find a possible cause of short time scale (<1 day) changes (±100 km/s) in the bulk speed of the solar wind observed by the M.I.T. solar wind experiment on IMP-7 and 8 within a stream. X-ray bright points, x-ray transients, and changes in area and boundaries within and around five central meridian passages of two coronal holes were examined. In all, five coronal hole crossings were studied. Levine's (1978) calculated field lines were used to give an estimate of the longitude and latitude on the sun of the field line connecting with the earth. For each crossing with sufficient x-ray coverage, there was a change in area of light regions, within the coronal holes, which occurred near the predicted magnetic field line connection point on the solar surface at the times that correspond to large changes in the bulk speed observed at the earth.

This work was supported in part by NASA contract NAS8-33137.

1. Spring Meeting 1982
2. SULL 004369 (Sponsor)
3. J. D. Sullivan
   37-675
   M.I.T.
   Cambridge, MA 02139
4. SS
5. None
6. 0
7. 0%
8. a. Daniel W. Calileo
      37-274
      M.I.T.
      Cambridge, MA 02139

   b. P. O. # SC-A-304728

   c. N/A
9. C